

1
2
3
4
5
6
7
8
9
10
11
12
13
14
15
16
17
18
19
20
21
22
23
24
25
26
27
28
29
30
31
32
33
34

Insights from Pb and O isotopes into along-arc variations in subduction inputs and
crustal assimilation for volcanic rocks in Java, Sunda arc, Indonesia

Heather K. Handley¹, Janne Blichert-Toft², Ralf Gertisser³, Colin G. Macpherson⁴, Simon P.
Turner¹, Akhmad Zaennudin⁵, Mirzam Abdurrachman⁶

¹Department of Earth and Planetary Sciences, Macquarie University, Sydney, NSW 2109, Australia.

²Laboratoire de Géologie de Lyon, Ecole Normale Supérieure de Lyon and Université Claude Bernard
Lyon 1, CNRS UMR 5276, 46 Allée d'Italie, 69007 Lyon, France.

³School of Physical and Geographical Sciences, Keele University, Keele, Staffordshire, ST5 5BG,
United Kingdom.

⁴Department of Earth Sciences, Durham University, Durham, DH1 3LE, United Kingdom.

⁵Center for Volcanology and Geological Hazard Mitigation (CVGHM), Geological Agency, Bandung
40122, Indonesia.

⁶Department of Geological Engineering, Bandung Institute of Technology, Bandung 40132, Indonesia.

*Corresponding author. Department of Earth and Planetary Sciences, Macquarie University,
Sydney, NSW 2109 Australia. Telephone: +61 2 9850 4403. Fax: +61 2 9850 8943. Email:
heather.handley@mq.edu.au

35 **Abstract**

36 New Pb isotope data are presented for Gede Volcanic Complex, Salak and Galunggung
37 volcanoes in West Java, Merbabu and Merapi volcanoes in Central Java and Ijen Volcanic
38 Complex in East Java of the Sunda arc, Indonesia. New O isotope data for Merbabu and new
39 geochemical and radiogenic isotope data (Sr-Nd-Hf-Pb) for three West Javanese, upper
40 crustal, Tertiary sedimentary rocks are also presented. The data are combined with published
41 geochemical and isotopic data to constrain the relative importance of crustal assimilation and
42 subducted input of crustal material in petrogenesis in Java. Also discussed are the significance
43 of limestone assimilation in controlling the geochemical and isotopic characteristics of
44 erupted Javanese rocks and the geochemical impact upon central and eastern Javanese arc
45 rocks due to the subduction of Roo Rise between 105-109°E. The negative correlation
46 between Pb isotopes and SiO₂, combined with mantle-like δ¹⁸O values in Gede Volcanic
47 Complex rocks, West Java, are most likely explained by assimilation of more isotopically-
48 primitive arc rocks and/or ophiolitic crust known to outcrop in West Java. The negative Pb
49 isotope-SiO₂ trend cannot be explained by assimilation of the known compositions of the
50 upper crustal rocks. A peak in δ¹⁸O whole-rock and mineral values in Central Javanese
51 volcanic rocks (Merbabu and Merapi) combined with along-arc trends in Sr isotope ratios
52 suggest that a different or additional crustal assimilant exerts control on the isotopic
53 composition of Central Javanese volcanic rocks. This assimilant (likely carbonate material) is
54 characterised by high δ¹⁸O and high Sr isotope ratio but is not particularly elevated in its Pb
55 isotopic ratio. Once the effects of crustal assimilation are accounted for, strong East to West
56 Java regional variations in Ba concentration, Ba/Hf ratio and Pb isotopic composition are
57 evident. These differences are attributed to heterogeneity in the subducted source input
58 component along the island: a more radiogenic Pb isotopic, lower Ba/Hf component (detrital-
59 rich subducted sediment) in West Java and a less radiogenic Pb isotopic, high Ba/Hf
60 component (attributed to a greater AOC/sediment fluid component and/or dominance of
61 pelagic, clay-rich subducted sediment) in East and possible Central Java. The subduction of
62 the Roo Rise, an area of oceanic basement relief, is thought to contribute significantly to the
63 spatial geochemical source input variations exhibited by Javanese volcanoes.

64

65 **1. Introduction**

66 Understanding the genesis of volcanic rocks in subduction zone settings is complicated by the
67 multitude of differentiation processes such as fractional crystallisation, magma mixing and

68 crustal assimilation and geochemical variations in source components, for example, the
69 mantle wedge, subducted oceanic crust and accompanying sediments or melts thereof, that
70 exert control on volcanic rock geochemistry (e.g., Davidson et al., 1987; Hildreth and
71 Moorbath, 1988; McCulloch and Gamble, 1991; Hawkesworth et al., 1991; Pearce and Peate,
72 1995). Furthermore, within-arc variations in crustal architecture and the nature (age and
73 composition) of the subducting slab and its associated sediments augment the difficulty of
74 disentangling differentiation effects on primary magmas from magma source characteristics.
75 Yet, in order to obtain an accurate understanding of element transfer in subduction zones, it is
76 of primary importance to identify shallow-level geochemical and isotopic modifications of
77 original source compositions in subduction zone petrogenesis.

78 The Java sector of the Sunda arc in Indonesia is the subject of a long-standing debate
79 on the relative importance of subduction input of crustal material versus magmatic interaction
80 with the surrounding arc crust in controlling the geochemistry of erupted volcanic rocks (e.g.,
81 Whitford, 1975; 1982; Wheller et al., 1987; Gasparon and Varne, 1998; Turner and Foden,
82 2001; Gertisser and Keller, 2003a; Chadwick et al., 2007; Handley et al., 2007; 2011;
83 Halldórsson et al., 2013). Early studies attributed a decrease in Sr isotope composition in
84 lavas from West Java to Bali to diminishing crustal assimilation as a result of eastward arc-
85 crustal thinning (Whitford, 1975; Hamilton, 1979). Gasparon and Varne (1998) also
86 suggested that crustal assimilation accounts for Sr, Pb and Nd isotope systematics along the
87 Sunda arc, from Sumatra to Lombok, relative to mid-ocean ridge basalt (MORB). In addition,
88 more recent detailed geochemical and isotopic studies on individual Javanese volcanoes
89 implicate an important role for crustal assimilation processes in the geochemical and isotopic
90 evolution of magma and its phenocrysts (e.g., Chadwick et al., 2007; Handley et al., 2008a;
91 Abdurrachman, 2012; Abdurrachman and Yamamoto, 2012; Troll et al., 2013). However,
92 addition of a subducted crustal component to the Java sector of the Sunda arc mantle wedge is
93 advocated by others to exert important control on the crustal signature observed within the
94 volcanic rocks (e.g., Whitford, 1982; Wheller et al., 1987; Edwards, 1990; Turner and Foden,
95 2001; Gertisser and Keller, 2003a; Handley et al., 2007; 2010; 2011). Wheller et al. (1987)
96 suggested that at least three geochemically and isotopically distinct source components are
97 involved in magma genesis: peridotitic mantle, subducted crustal input and a K-group-rich,
98 low-Sr isotope, mantle-derived component. Edwards et al. (1993) used B/Be and radiogenic
99 isotopes of seven volcanic centres along the Sunda and Banda arc (including Guntur and
100 Cereme from the volcanic front in Java) to suggest that the composition of the subduction
101 input is homogenous along the Sunda arc. In contrast, Handley et al. (2011) argued for along-

102 arc heterogeneity in this component in Java based primarily on Nd-Hf isotope compositions
103 of the volcanic rocks. A recent chemical and isotope (He-C-N) study of active fumarole and
104 hydrothermal gas and water by Halldórsson et al. (2013) proposed that the major volatile
105 budget of the western Sunda arc (Sumatra, Java and Bali) is dominantly sourced from
106 subduction input of crustal material rather than magmatic interaction with thick/old crustal
107 basement.

108 Considering the nature of the debate, it is surprising that only relatively few Pb isotope
109 data are available for Javanese volcanic rocks. The significant contrast in Pb concentration
110 and isotopic composition of the mantle relative to marine and continental sediments (e.g.,
111 Sun, 1980; Price et al., 1986; Ben Othman et al., 1989; Rehkämper & Hofmann, 1997;
112 Gasparon and Varne 1998; Chauvel and Blichert-Toft, 2001) dictates that Pb isotopic ratios of
113 mantle-derived magma are highly sensitive to the addition of subduction-related and/or
114 assimilated arc crustal material during volcanic rock petrogenesis (e.g., James, 1982;
115 Whitford, 1982; Miller et al., 1994; Carpentier et al., 2008). Previously published Pb isotope
116 data of Javanese volcanoes are largely confined to studies analysing only one or two samples
117 from each volcano, with the data amalgamated in broad arc overviews (Whitford, 1982;
118 Turner and Foden, 2001; Woodhead et al., 2001). Prior to this study, only Guntur and Merapi
119 volcanoes have five or more samples with published Pb isotope analyses (Edwards, 1990;
120 Gertisser and Keller, 2003a). Yet, to understand the contribution of crustal assimilation and
121 the nature of assimilants, it is essential to have tight constraints on differentiation
122 characteristics at individual volcanoes.

123 The oxygen isotope compositions of subduction zone volcanic rocks can also yield
124 key information on crustal assimilation processes during magmatic differentiation and
125 therefore, help to discriminate between subduction-related and assimilated arc crustal inputs.
126 This is due to the significant contrast between the low and relatively constant $\delta^{18}\text{O}$ values in
127 the upper mantle ($+5.5 \pm 0.2\text{‰}$ (Eiler, 2001) to $+5.7 \pm 0.2\text{‰}$ (Harmon and Hoefs, 1995) in
128 MORB relative to Standard Mean Ocean Water (SMOW)) and generally high $\delta^{18}\text{O}$ values of
129 upper crustal materials (typically $>10\text{‰}$; e.g., Ito and Stern, 1986; Davidson and Harmon,
130 1989) that have undergone low temperature interaction with meteoric water. Oceanic
131 lithosphere may have low and moderately high $\delta^{18}\text{O}$ values (typically between 3-10‰)
132 depending on whether high-temperature hydrothermal alteration or low-temperature alteration
133 and weathering of rocks occurred. Normal depth profiles of oceanic lithosphere show ^{18}O -

134 enriched pillow lavas and ^{18}O -depleted sheeted dikes and uppermost gabbros (Gao et al., 2006
135 and references therein).

136 Here we present new whole-rock Pb isotope data for volcanoes in West Java (Salak,
137 Gede Volcanic Complex and Galunggung), Central Java (Merbabu and Merapi) and East Java
138 (Ijen Volcanic Complex) (Fig.1). New whole-rock oxygen isotope data are presented for
139 Merbabu volcano and new geochemical and radiogenic isotope (Pb, Sr, Nd, Hf) data for three
140 West Javanese Neogene sedimentary rocks of varied lithology are also presented. The new
141 volcano Pb isotope data are combined with previously published geochemical and isotopic
142 data for the same samples (Turner and Foden, 2001; Gertisser and Keller, 2003a; Handley et
143 al., 2007; 2008a; 2010; 2011) and with other published Javanese volcanic rock data to
144 increase our understanding of the relative importance of both crustal assimilation and
145 subduction input of crustal material in Sunda arc volcanic petrogenesis. This study also aims
146 to provide insight into the nature of the underlying arc crust involved in crustal assimilation
147 and thereby expose likely transitions in the composition of the arc basement in Java. We show
148 that through detailed studies of individual volcanoes it is possible to resolve 'shallow' versus
149 'deep' crustal inputs in arc magma genesis and we discern the geochemical and isotopic
150 modification of mantle wedge source compositions by both crustal assimilation and subducted
151 crustal input in volcanic petrogenesis in Java.

152

153 **2. Tectonic and geological setting**

154 The Sunda arc, stretching from the Andaman Islands north-west of Sumatra, through Java to
155 Flores in the Banda sea is part of the Indonesian subduction zone system, formed by
156 subduction of the Indo-Australian plate beneath the Eurasian Plate at a rate of $\sim 6\text{-}7\text{ cm yr}^{-1}$
157 (Le Pichon, 1968; DeMets et al., 1990; Tregoning et al., 1994; Fig. 1a). The tectonic setting
158 of the Indonesian region is described in detail in Hamilton (1979) and Hall (2002; 2011). The
159 Sunda arc basement is thought to be made up of a series of Gondwanan lithospheric
160 fragments that were accreted to the pre-Cretaceous (Sundaland) Eurasian Plate margin in the
161 Cretaceous (e.g., Metcalfe, 1990; Wakita, 2000; Hall, 2011; Fig. 1a). The associated
162 Cretaceous accretionary-collisional complexes are exposed in Central and West Java (Fig.
163 1a). The Luk Ulo complex near Karangsambung in Central Java consists of ophiolitic rocks
164 (mafic and ultramafic rocks), sedimentary rocks, and crystalline schists and gneisses
165 occurring as tectonic slabs in a black-shale matrix tectonic *mélange* (Wakita et al., 1994;
166 Kadarusman et al., 2007 and references therein). Such complexes are also exposed at Ciluteh
167 in West Java and Jiwo Hills in Central Java (Metcalfe, 1990; Wakita, 2000; Fig. 1a).

168 However, the majority of exposed rocks on Java consist of younger, Cenozoic sedimentary
169 sequences and volcanic arc rocks (e.g., van Bemmelen, 1949; Hamilton, 1979; Clements et
170 al., 2009). A major structural feature and geological division is inferred between Central and
171 East Java, running ~NE-SW through the island, close to Merapi at the volcanic front and
172 Muria volcano at the rear arc (Fig. 1b). This lineament is described as either the strike-slip
173 Central Java Fault (Chotin et al., 1984; Hoffmann-Rothe et al., 2001) or the inferred Progo-
174 Muria lineament (Smyth et al., 2005; Smyth et al., 2007) and is suggested to mark the eastern
175 limit of accreted Cretaceous terranes and sutures (Hoffmann-Rothe et al., 2001) or western
176 limit of Archean-aged zircons in the southern mountains (Smyth et al., 2007), respectively.
177 Handley (2006) also proposed a significant crustal boundary at this location (between Merapi
178 and Kelut) based on a compilation of volcanic Sr isotope data, volcano activity and volcano
179 morphology. East of Merapi, the topography along the volcanic front changes from the deeply
180 dissected mountainous and more rugged topography of West and Central Java to the relatively
181 flat East Javan topography, punctuated by large conical volcanoes with relatively smooth
182 volcanic slopes (Handley, 2006; Fig. 1c). Wheller et al. (1987) suggested that the area
183 between Merapi and Kelut is an extinct sector of the arc, containing the volcanoes of Wilis
184 and Lawu, which only display solfataric activity. Recent work highlighting the structural
185 complexity of the Java crust is detailed in Smyth et al. (2007) and Clements et al. (2009).

186 The subducting plate also shows variability along the arc. The age of the subducting
187 Indian Ocean crust increases from West (~80 Ma) to East Java (~130 Ma) (Fig. 2; Hamilton,
188 1979; Syracuse and Abers, 2006), while the dip angle of the slab decreases slightly from 50°
189 to 42° (Syracuse and Abers, 2006). The location of the volcanoes in relation to the slab depth,
190 H , and distance from the trench varies quite dramatically along the Java sector of the arc
191 (Figs. 2c and d) but unlike slab age and dip, slab depth does not show a simple increase or
192 decrease along strike (Hutchison, 1982; Syracuse and Abers, 2006). The vertical depth to the
193 slab and the horizontal distance to the trench increase from Krakatau to Ungaran/Dieng
194 volcanoes (~110°E) then abruptly decrease to Wilis, Lawu and Kelut (~112°E) before
195 increasing again to Ijen (114°E). The relatively systematic decrease in slab dip from West to
196 East Java (Fig. 2b) rules out significant lateral slab-tear as an explanation for the variation in
197 slab depth (cf. Garwin et al., 2005). A recent study using Hough Transform analysis of
198 volcano positions in Java suggests that stress regimes in the arc lithosphere control the spatial
199 distribution of the volcanoes (Pacey et al., 2013). Present day collision and subduction of the
200 Roo Rise between 109°E and 115°E (Fig. 1b), an area of oceanic basement relief, has caused
201 dramatic changes in the character of the Java plate margin and a transition from subduction

202 accretion (west of $\sim 109^\circ\text{E}$ at the Java Trench) to subduction erosion (east of $\sim 109^\circ\text{E}$ at the
203 Java Trench) (Kopp et al., 2006). This is manifest in a marked change from a thick
204 accretionary wedge, continuous outer forearc high and sediment filled trench in the west to no
205 distinct frontal prism or continuous outer forearc high and displacement of the trench and
206 deformation front by ~ 60 km to the north in the east. The northward displacement of the
207 trench is observed between 109°E and 115°E (Kopp et al., 2006), corresponding across strike
208 to volcanoes in Central and East Java. The composition and mass of sediment in the Java
209 Trench also vary along the Java sector. Plank and Langmuir (1998) proposed that 300 m of
210 sediment is subducted beneath Java. Up to 5 km of sedimentary material fills the Sumatra
211 Trench, less than 1 km exists in the western Java Trench and virtually no trench sediments are
212 present in the eastern Java Trench (Plank and Langmuir, 1998; Kopp et al., 2006). The thicker
213 sedimentary deposits present at the site of subduction in West Java, compared with East Java,
214 are a result of the closer proximity of West Java to turbiditic material sourced from the
215 Himalayan collision zone and deep-sea fans surrounding India (Plank and Langmuir, 1998).
216 Sediments deposited on the Indian Ocean Plate south of the trench are relatively uniform in
217 thickness along the arc (200-400 m) (Hamilton, 1979; Moore et al., 1980) and are dominantly
218 detrital-poor, pelagic sediments (Hamilton, 1979).

219

220 **3. Sample selection and data presentation**

221 To facilitate investigation of differentiation processes and source compositions, samples were
222 selected for Pb isotope analysis from West (Salak and Gede Volcanic Complex), Central
223 (Merbabu) and East (Ijen Volcanic Complex) Javanese volcanoes (Fig. 1c) for which there is
224 no prior published Pb isotope data but for which geochemical and other isotope (Sr-Nd-Hf
225 and some O) data exist (Handley et al. 2007; 2008a; 2010; 2011). To assist in constraining
226 crustal assimilation processes, the sub-sets of samples selected span the full range in SiO_2
227 content measured at each volcano. New Merapi (Central Java) samples were analysed from
228 the 2006 and 2010 eruptions. Additional samples from Galunggung and Merapi volcanoes
229 were selected that have previously published thermal ionisation mass spectrometry Pb isotope
230 data. These samples were re-analysed in this study to facilitate comparison between data sets
231 collected in different laboratories using different methods and instrumentation (e.g., Tl-doped
232 multi-collector inductively-coupled plasma mass spectrometry (MC-ICP-MS) with sample-
233 standard bracketing data versus un-spiked, conventionally fractionation-corrected thermal
234 ionisation mass spectrometry (TIMS) data). The Pb isotope data comparison is provided in
235 the Appendix along with further details about the selection of previously published Javanese

236 data sets for Pb isotope data comparison in this study. New whole-rock oxygen isotope data
237 are presented for Merbabu for which there was no previously published O isotope data. The
238 new Javanese volcano Pb and O isotope data are displayed in Tables 1 and 2, respectively.
239 Samples from Gede Volcanic Complex include volcanic rocks from the main Gede edifice,
240 twin volcanic centre Pangrango (n = 1), nearby Gegerbentang vent (n = 1) and Older
241 Quaternary volcanoes (n = 1; Table 1). Samples from Salak include those from both the
242 central vent and flank vents and a Pre-Salak pumice sample (S100). Those from Ijen Volcanic
243 Complex include volcanic rocks from the caldera-rim and intra-caldera eruptive centres
244 (Table 1). Little geochemical and isotopic information is available for upper crustal rocks in
245 West Java. Therefore, three West Javanese upper crustal, Tertiary sedimentary rocks have
246 been analysed (major element and trace element and Pb-Sr-Nd-Hf isotopic compositions;
247 Tables 1 and 3). A calcareous sediment/marl (SED-A), a volcanoclastic sandstone (SED-B)
248 and a mudstone (SED-C) were collected from a river valley near the Bukit Pelangi golf
249 course, approximately 10 km east of Bogor and 20 km NW of the summit of Gede volcano
250 (Fig. 1c, Table 3). The sedimentary units dip between 20-30 degrees to the south-south west,
251 towards Gede volcano. Abundant planktic foraminifera (*Globigerinoides* and *Orbulina*) in the
252 marl suggest a Neogene (likely, upper Miocene or younger) age for the rocks. These data
253 provide information on the likely character of potential crustal assimilants in West Java and
254 particularly at Gede volcano.

255 The island of Java and the strike of subduction, as indicated by the Java Trench, are
256 oriented approximately east-west. Therefore, the longitude of the volcano is used to represent
257 volcano position along the arc. As across-arc changes in chemistry are recognised at the
258 Sunda arc (Rittman, 1953; Whitford and Nicholls, 1976; Hutchison, 1976; Edwards, 1990)
259 the rear-arc volcanoes of Muria (370 km above the Wadati-Benioff zone (WBZ) in Central
260 Java) and Ringgit Beser (210 km above the WBZ in East Java) (Fig. 1c) are excluded from
261 data comparison. One of the two Merapi samples analysed by Woodhead et al. (2001)
262 displays anomalously low Pb isotope ratios relative to the other Merapi Pb isotope data and to
263 the Central Java group. This sample, therefore, has not been plotted on the figures or
264 considered in the discussion.

265 To facilitate the identification of geochemical trends, volcanoes are grouped into
266 West, Central and East Javanese provenance (Fig. 1c). Accordingly, the West Java group
267 includes volcanoes from Danau to Cereme, the Central Java group from Slamet to Merapi and
268 the East Java group from Lawu to Ijen (Fig. 1). Slamet, the westernmost Central Java
269 volcano, shows several geochemical similarities to West Java (e.g., lower Ba concentration

270 and Ba/Hf ratio) yet displays high Sr isotope ratios similar to other Central Java volcanoes
271 and, therefore, has been grouped with Central Java. The placing of Lawu and Wilis is
272 uncertain, whether Central or East Java, as there is limited geochemical and, particularly,
273 isotopic data available. Morphologically, these volcanoes are similar to other East Java
274 volcanoes (single, large composite volcanoes) and lie to the east of the Central Java
275 Fault/Progo-Muria lineament and hence have been placed in the East Java Group. Due to the
276 multiple spellings of Javanese volcano names, those used are consistent with the spellings
277 given the Global Volcanism Program database (<http://www.volcano.si.edu/index.cfm>).

278

279 **4. Analytical techniques**

280 Lead isotope ratios for Salak, Gede, Galunggung, Merapi and Ijen volcanic rocks and the
281 three West Java sedimentary rocks were determined on bulk-rock powders by wet chemistry
282 and multi-collector inductively-coupled plasma mass spectrometry (MC-ICP-MS; Nu Plasma
283 500 HR) using Tl doping and sample-standard bracketing (White et al., 2000) at the Ecole
284 Normale Supérieure in Lyon. Details of the preparation of rock powders can be found in
285 Turner and Foden (2001), Gertisser and Keller (2003a), Handley et al. (2007; 2008a; 2010;
286 2011) and Preece et al. (2013). The whole-rock powders were first leached in hot 6 M HCl
287 prior to attack in a 3:1:0.5 mixture of concentrated HF:HNO₃:HClO₄. The samples were then
288 taken up in 6 M HCl after fuming with HClO₄ to eliminate fluorides. Lead was separated by
289 ion-exchange chromatography on 0.5 mL columns filled with Bio-Rad AG1-X8 (100-200
290 mesh) resin using 1 M HBr to first elute the sample matrix followed by 6 M HCl to
291 subsequently recover the Pb. The total procedural Pb blank was < 20 pg. The NIST 981 Pb
292 standard and the values of Eisele et al. (2003) were used for bracketing the unknowns (every
293 two samples), and Tl was used to monitor and correct for instrumental mass bias. Internal
294 uncertainties on the reported Pb isotope ratios are 50-100 ppm. The Pb isotope data are listed
295 in Table 1.

296 The Merbabu Pb isotope measurements were carried out on bulk-volcanic rock
297 powders without further pre-treatment at the University of Tübingen using analytical methods
298 described in detail by Hegner et al. (1995a, 1995b). The preparation of rock powders follows
299 that detailed in Gertisser and Keller (2003a). Lead was separated on Teflon columns
300 containing 80 µl AG 1-X8, 100-200 mesh and employing a HBr-HCl wash and elution
301 procedure. Lead isotope compositions were determined by thermal ionisation mass
302 spectrometry on a Finnigan MAT 262 mass spectrometer in static collection mode. Lead was
303 loaded with a Si-gel onto a pre-conditioned Re filament and measured at 1250-1300°C. Total

304 procedure blanks were < 50 pg. A factor of 0.1% fractionation per mass unit was applied to
305 all Pb isotope analyses, using NBS SRM 982 as the reference material and NBS SRM 981 as
306 a standard. The estimated 2σ uncertainty of the reported Merbabu volcano Pb isotope ratio is
307 better than 0.01 %.

308 Merbabu whole-rock oxygen isotope ratios were measured using a Finnigan MAT 252
309 gas source mass spectrometer (Hegner et al., 1995b). Silicate oxygen was extracted by
310 bromine pentafluoride at 600°C, followed by conversion to CO₂. The results are reported as
311 per mil (‰) deviations relative to Standard Mean Ocean Water (SMOW) and refer to a
312 certified value of $9.6 \pm 0.1\%$ measured on NBS 28. For the O isotope determinations at least
313 two measurements were performed for a given sample and the average $\delta^{18}\text{O}$ values are
314 reported in Table 2. All values were reproduced within an analytical error of 0.1-0.2‰.

315 The major element, trace element and Sr–Nd–Hf isotopic data for the West Java
316 sedimentary rocks were collected using the same procedures and data quality constraints as
317 those given in Handley et al. (2010) and Handley et al. (2011). Full details on the analytical
318 techniques for the West Java sedimentary rocks are provided in the Appendix.

319

320 **5. Results**

321 *5.1. Pb isotope data*

322 The new Pb isotope data for volcanic rocks from Salak, Gede Volcanic Complex,
323 Galunggung, Merbabu, Merapi and Ijen Volcanic Complex are presented in Table 1 and Fig.
324 3. The new data (colour-filled symbols in Figs. 3a and b) form a positive array in $^{207}\text{Pb}/^{204}\text{Pb}$
325 and $^{208}\text{Pb}/^{204}\text{Pb}$ versus $^{206}\text{Pb}/^{204}\text{Pb}$ space and display higher Pb isotope ratios than Indian
326 Ocean mid-ocean ridge basalt (I-MORB) and seamounts subducting at the Java Trench,
327 represented by the Eastern Wharton Basin and Argo Basin Volcanic Provinces (I-Seamount
328 East). Most of the Javanese volcanic rock data overlap with the fields for local Indian Ocean
329 subducted sediments (I-SED), Indian Ocean Mn crusts and to a lesser extent, the limited data
330 available for the local upper crust (Sumatran intrusive rocks (Intrusive), calcareous sediment
331 upper crust samples from Central Java and the new West Java upper crust samples (Local
332 Crust)). Ijen volcanic rocks have the most primitive Pb isotopic compositions, with most
333 displaying less radiogenic ratios than local subducted sediment and local upper crustal
334 sedimentary rocks (Local Crust). The Gede volcanic rocks exhibit the most radiogenic values
335 for Javanese volcanoes so far determined (Figs. 3c and d), with the associated centres of
336 Pangrango and Gegerbentang displaying the highest Pb isotopic ratios (Table 1). Salak and
337 Galunggung show a similar range in Pb isotope ratios, overlapping with the more primitive

338 end of the Gede data array. The new data for Merapi (n = 13, Table 1) which consists of both
339 high-K (< 1900 ¹⁴C y B.P.) and medium-K (> 1900 ¹⁴C y B.P.) rock types (Gertisser and
340 Keller, 2003b) and recently erupted 2006 and 2010 volcanic rocks, show remarkable within-
341 suite homogeneity in Pb isotopic composition compared to the other volcanoes. However, the
342 Merapi rocks lie slightly elevated, relative to the main Java trend, at higher ²⁰⁷Pb/²⁰⁴Pb for a
343 given ²⁰⁶Pb/²⁰⁴Pb (Fig. 3c). The Pb isotope ratios of Merbabu volcanic rocks from Central
344 Java overlap with the data for Salak and Gede.

345 The local, upper crustal, sedimentary rocks from West Java display relatively similar
346 Pb isotopic compositions to one another and lie at intermediate Pb isotopic ratios relative to
347 the Javanese volcanic rocks (Figs. 3c and d). The sedimentary rocks exhibit more primitive
348 isotopic ratios than Gede Volcanic Complex rocks and more radiogenic values than Ijen
349 Volcanic Complex. In ²⁰⁸Pb/²⁰⁴Pb-²⁰⁶Pb/²⁰⁴Pb space, the marl and mudstone rocks lie slightly
350 off the main Javanese volcanic rock trend, at lower ²⁰⁸Pb/²⁰⁴Pb for a given ²⁰⁶Pb/²⁰⁴Pb.

351

352 5.2. Oxygen isotope data

353 New bulk-rock oxygen isotope data of Merbabu volcano are presented in Table 2 and Fig. 4.
354 Merbabu δ¹⁸O values range from +6.4 to +8.4‰, are higher than typical values for MORB of
355 +5.5 ± 0.2 ‰ (Eiler, 2001) and +5.7 ± 0.2 ‰ (Harmon and Hoefs, 1995) and extend to the
356 highest volcanic whole-rock δ¹⁸O values yet reported for Java. The Merbabu δ¹⁸O values
357 largely overlap with the range in whole-rock values reported for neighbouring Merapi volcano
358 and Cereme, West Java (insets to Figs. 4a and b), which also display higher overall δ¹⁸O
359 values relative to δ¹⁸O bulk volcanic rock data of Galunggung (Figs. 4a and b). Low loss on
360 ignition (LOI) values in the Merbabu volcanic rocks of -0.44 to 0.71 wt%, except for MB-6
361 with a higher LOI value of 1.12 wt% (Handley et al., 2011), suggest that post-eruption
362 secondary alteration processes, such as weathering, have not significantly affected the rocks
363 and by inference, the measured oxygen isotope values. The samples with the highest δ¹⁸O
364 values (MB-16 and MB22) do not correspond to the sample with the highest LOI (MB-6).
365 The Merbabu δ¹⁸O values are much lower than those of the local calcareous sedimentary
366 rocks given by Gertisser and Keller (2003a) (+18.9 to 20.5‰), and local limestone samples of
367 Troll et al. (2013) (+24.0 to 24.5‰), and also lower than values measured in local
368 volcanoclastic crust (+12.5; Troll et al., 2013) and bulk calc-silicate xenoliths found within
369 Merapi lavas (+11.5 to 14.2‰; Gertisser and Keller, 2003a; Troll et al., 2013). Note that the
370 calc-silicate xenolith δ¹⁸O values likely represent the resultant limestone-magma interaction

371 rather than the carbonate protolith. The highest Merbabu $\delta^{18}\text{O}$ values correspond to the
372 samples with the lowest Pb isotope ratios (Fig. 4a inset).

373

374 **6. Discussion**

375 It is widely considered that the majority of Javanese arc magmas are formed through flux-
376 melting of the mantle wedge due to subduction of the Indo-Australian Plate beneath the
377 Eurasian plate (e.g., Harmon and Gerbe, 1992; Gertisser and Keller, 2003a; Handley et al.,
378 2007; 2011). Although, the low volatile contents measured in mafic glass inclusions in high-
379 magnesium basalts from Galunggung, led Sisson and Bronto (1998) to suggest that pressure-
380 release melting of hot mantle peridotite may play a role in magma genesis for some Javanese
381 volcanoes. Upon ascent to the surface, the major and trace element composition of magmas
382 may be modified by a number of processes such as fractional crystallisation, magma mixing
383 and crustal assimilation (e.g., Anderson, 1976; Sakuyama, 1979; DePaolo, 1981; Thirlwall et
384 al., 1996). Yet, the radiogenic isotopic composition of a magma is not expected to change by
385 recent partial melting and fractional crystallisation or magma mixing, provided that the mixed
386 magmas are from the same source. However, the isotopic ratios of magma are susceptible to
387 modification by assimilation of crustal material during ascent and shallow-level storage, if the
388 magma and assimilated material are characterised by contrasting isotopic ratios (e.g.,
389 Davidson et al., 2005). Similarly, stable O isotope values of mantle-derived melts may be
390 significantly modified by assimilation of crustal material that has experienced low-
391 temperature interaction with meteoric water or seawater, or interaction with high-temperature
392 hydrothermal fluids (e.g., James, 1981; Bindeman et al., 2001). Therefore, the new Pb and O
393 isotope data presented here can be used to elucidate the relative role that crustal assimilation
394 has exerted on magma chemistry during differentiation of Javanese rocks as a means to “see
395 through” to source input variations.

396

397 *6.1. Pb isotopic evidence for assimilation of crustal material*

398 Owing to the large contrast in Pb concentration and Pb isotopic composition between mantle-
399 derived magma (low concentration and less radiogenic) and continental upper crust (high
400 concentration and more radiogenic) the former is sensitive to incorporation of crustal material
401 during differentiation in the arc crust (e.g., Davidson, 1987). If assimilation is concomitant
402 with fractional crystallisation of magma (AFC) (e.g., DePaolo, 1981), evidence for
403 assimilation may be visible through correlations of isotope ratios with indices of
404 differentiation (e.g., SiO_2 , MgO).

405 The plot of $^{207}\text{Pb}/^{204}\text{Pb}$ versus SiO_2 content for Javanese volcanic rocks (Fig. 5)
406 highlights the significantly higher $^{207}\text{Pb}/^{204}\text{Pb}$ for West (Gede, Salak, Galunggung) and
407 Central (Merbabu, Merapi) Java compared to East Java (Ijen) at similar degrees of magmatic
408 differentiation. The Pb isotope ratios of Ijen volcanic rocks do not correlate with indices of
409 differentiation, though they do show some degree of scatter. The volcanic rocks from Salak
410 show no clear correlation despite inferred crustal assimilation at this centre based on the
411 modelling of trace elements and Sr isotope ratios of the Central Vent Group (CVG) (Handley
412 et al., 2008a). This may be due to the slightly more limited number of CVG samples analysed
413 for Pb isotopes ($n = 3$; Table 1) compared to those analysed for Sr isotopes ($n = 5$). Negative
414 correlations between Pb isotope ratios and SiO_2 are observed for Merbabu ($R^2 = 0.85$) and
415 Gede Volcanic Complex ($R^2 = 0.71$), suggesting the incorporation of isotopically contrasting
416 material at these volcanoes during magmatic differentiation. The correlations observed for
417 Merbabu and Gede show that the lowest SiO_2 content rocks, inferred to represent the least
418 differentiated samples, have the most radiogenic Pb isotopic compositions. The three analyses
419 available for Galunggung also suggest a similar, negative trend. Two possible hypotheses for
420 the observed negative trends are: 1) increasing incorporation of less radiogenic material, such
421 as more isotopically primitive arc rocks or ophiolitic oceanic crust (now in the arc crust),
422 during progressive magmatic evolution or, 2) the lowest silica rocks have assimilated the
423 most (by volume) radiogenic crustal material. The exposed arc basement in West and Central
424 Java is composed of accreted Mesozoic ophiolitic and arc rocks and Eocene to Late Miocene
425 volcanogenic turbidites and breccias, quartz-rich sandstones and limestone (Clements and
426 Hall, 2007; Section 2). The observed negative Pb isotope trends of Gede and Merbabu
427 volcanic rocks may, therefore, be explained by hypothesis one, whereby progressive
428 assimilation of less radiogenic mafic-ultramafic (ophiolitic-type) or more primitive arc
429 basement occurs during magmatic differentiation (Fig. 5). A similar model has been proposed
430 for Lopevi volcano in the intra-oceanic Vanuatu arc, where negative correlations between Sr
431 isotope ratios and SiO_2 content are observed (Handley et al., 2008b). With regard to the
432 second hypothesis, there are two further possibilities: a) the higher temperature and lower
433 viscosity of the more primitive, lower SiO_2 magma enabled assimilation of a greater volume
434 of crust, relative to more evolved magma (e.g., Huppert and Sparks, 1985; Peccerillo et al.,
435 2004) or b) the negative Pb isotope correlation observed for Gede and Merbabu is explained
436 by assimilation of a component characterised by low SiO_2 content and high Pb isotope ratios
437 such as limestone/calcareous sediment. Assimilation of limestone has already been suggested
438 as an important process during magmatic evolution at Merapi volcano (Chadwick et al., 2007;

439 Deegan et al. 2010; Troll et al., 2013), adjacent to Merbabu. Limestone sampled from a
440 carbonate platform at Parangtritis, south of Merapi, has low SiO₂ (0.28 wt %), Na₂O (0.12 wt
441 %) and K₂O (0.00 wt %) contents and high CaO and CO₂ contents (Deegan et al., 2010) but
442 unfortunately, Pb isotope data are not available for these samples. However, the Pb isotope
443 composition of a local, low SiO₂ content, West Javanese calcareous marl (SED-A, Tables 1
444 and 3) collected 20 km NE of the summit of Gede volcano in West Java and two calcareous
445 marls collected from the Wonosari Beds, Southern Mountains, south-east of Imogiri
446 (Miocene) and Djiwo Hills, south of Klaten (Eocene), relatively close to Merbabu and Merapi
447 in Central Java (Gertisser and Keller, 2003a) have lower Pb isotope ratios than the majority of
448 West and Central volcanic rocks (Figs. 3 and 5). Therefore, crustal assimilation of the local
449 calcareous sedimentary rocks (analysed to date) cannot explain the high Pb isotope ratios of
450 the West and Central Javanese rocks in the lowest SiO₂ samples (Fig. 5) or the observed
451 correlation between ²⁰⁷Pb/²⁰⁴Pb and SiO₂.

452 To further investigate the potential control of carbonate assimilation on the whole-
453 rock geochemical composition of Javanese volcanic rocks, experimental research carried out
454 on carbonate assimilation at Italian volcanoes can be utilised. Experimental work on the
455 interaction between limestone and magma in connection with Italian volcanoes has shown
456 that assimilation of limestone creates a negative correlation between Na₂O + K₂O and SiO₂,
457 or a horizontal array at low SiO₂ contents. The experimental data trends (shown as arrows on
458 Fig. 6) agree well with melt inclusion data of volcanic rocks at Vesuvius volcano (Iacono
459 Marziano, 2008). Figure 6 shows an overall positive correlation in Na₂O + K₂O versus SiO₂
460 space for the Javanese data set and, more importantly, a strong positive correlation for Gede
461 ($R^2 = 0.76$) and a slightly weaker correlation for Merbabu ($R^2 = 0.58$). This suggests that,
462 unlike Vesuvius, limestone assimilation or assimilation of local calcareous sediments (SED-
463 A, Table 3) does not fully control the major element composition of most Javanese volcanic
464 rocks. Furthermore, the range in silica content observed at Gede and Merbabu is comparable
465 to the other Javanese volcanoes (e.g., Ijen) and is not significantly lower as might be expected
466 if significant limestone/carbonaceous sediments were being assimilated. The Central Javanese
467 volcanoes do show relatively more scatter in intra-volcanic trends and higher Na₂O + K₂O for
468 a given SiO₂ content compared to West Javanese rocks suggesting a potential possible role for
469 some degree of carbonate assimilation in Central Java relative to West Java but does not
470 dominate the whole-rock geochemical composition of the erupted rocks. Alternatively, the
471 Central Javanese volcanoes are located at greater distance from the trench and subducting slab
472 (Fig. 2), which may explain their generally higher K₂O content.

473 The new Pb isotope data of Merapi volcanic rocks, provide two surprising
474 observations. Firstly, that there is little difference in the Pb isotope ratio between the
475 temporally divided medium-K and high-K rock groups (Table 1; Gertisser and Keller, 2003a).
476 Secondly, that despite strong evidence for crustal contamination by carbonate/more
477 radiogenic material from the Sr isotope, crystal stratigraphy study of Chadwick et al. (2007),
478 the volcano displays an extremely limited within-suite range in whole-rock Pb isotopic
479 composition. This is particularly noticeable when compared to the within-suite range
480 observed at Gede, Salak and Ijen. The Merapi samples lie at higher Pb isotope compositions
481 than the available Pb isotope data for local calcareous crustal rocks (Figs. 3 and 5) and lie
482 slightly off the main Java array, at elevated $^{207}\text{Pb}/^{204}\text{Pb}$ for a given $^{206}\text{Pb}/^{204}\text{Pb}$. Greater
483 knowledge of the Pb isotopic compositional range of the local crust, including carbonaceous
484 sediments is required in order to fully determine the cause of the displacement of Merapi data
485 from the main Java trend an apparent buffering of the volcano's Pb isotope composition.

486 In summary, the Pb isotope data show evidence for crustal assimilation processes at
487 Gede and Merbabu (and possibly Galunggung). The negative correlation between Pb isotope
488 ratio and SiO_2 content suggests either that the more mafic, higher temperature rocks have
489 assimilated the most (by volume) radiogenic crustal material, or that the crustal assimilant is
490 characterised by a lower Pb isotopic composition relative to the source magma. These options
491 are discussed further below using constraints from O isotopes and trace element data. The Pb
492 isotope compositions of the volcanic rocks and local crustal rocks from West and Central
493 Java, combined with $\text{K}_2\text{O} + \text{Na}_2\text{O}$ versus SiO_2 volcanic data trends suggest little importance
494 of the assimilation of carbonaceous material at Gede. The overall higher $\text{K}_2\text{O} + \text{Na}_2\text{O}$
495 contents and more scattered data trend in $\text{K}_2\text{O} + \text{Na}_2\text{O}$ - SiO_2 space for Merbabu, relative to
496 Gede, suggest potentially a limited role for the assimilation of carbonaceous material.
497 However, to date, the Pb isotope ratios available for local carbonaceous crustal rocks do not
498 provide high enough Pb isotope ratios to be suitable contaminant end members to support this
499 model. The lower Pb isotopic ratios in Ijen volcanic rocks, compared to Central and West
500 Java, do not correlate with indices of differentiation indicating that assimilation of
501 isotopically distinct crustal material is not an important process in modifying magma isotopic
502 compositions at this volcano.

503

504 *6.2. Oxygen isotope constraints on crustal assimilation*

505 Oxygen isotope data can be utilised to further investigate the suggested importance of crustal
506 assimilation at Merbabu and Gede gained from Pb isotope data. The new Merbabu whole-

507 rock $\delta^{18}\text{O}$ data are significantly higher than typical values for MORB ($+5.7 \pm 0.2\%$, Harmon
508 and Hoefs, 1995 and $+5.5 \pm 0.2\%$, Eiler, 2001) (Table 2; Fig. 4) suggesting possible
509 interaction between magma and upper crustal material that has undergone low-temperature
510 interaction with meteoric water. The Merbabu $\delta^{18}\text{O}$ values are similar to the elevated whole-
511 rock $\delta^{18}\text{O}$ values of Merapi, which also displays elevated plagioclase and clinopyroxene $\delta^{18}\text{O}$
512 values (Fig. 4) and for which crustal assimilation processes have been implicated (Gertisser
513 and Keller, 2003a; Chadwick et al., 2007). The two highest $\delta^{18}\text{O}$ values are found in the
514 lowest Pb isotope rocks (Fig. 4a) suggesting that the assimilant may be characterised by lower
515 Pb isotope ratios than the ascending magma.

516 The previously published olivine and clinopyroxene O isotope mineral separate data
517 from Gede Volcanic Complex possess relatively restricted $\delta^{18}\text{O}$ values and lie largely within
518 error of mantle $\delta^{18}\text{O}$ values (Figs. 4b and c; Handley et al., 2010). These values suggest that
519 the assimilant involved has not significantly interacted with low-temperature fluids and,
520 therefore, assimilation may occur relatively deep in the crust, and/or, that the assimilant is
521 characterised by low $\delta^{18}\text{O}$ values. The latter is consistent with assimilation of more primitive
522 arc rocks and/or ophiolitic material, which was suggested as a possible explanation for the
523 negative correlation between Pb isotope ratios and SiO_2 contents of the volcanic rocks. The
524 Gede samples for which both clinopyroxene O isotope data and whole-rock Pb data are
525 available show no correlation between stable and radiogenic isotopes (Figs. 4a and 4c).

526 Although mineral O isotope data are not available for Merbabu lavas, taking all
527 published Javanese plagioclase and clinopyroxene $\delta^{18}\text{O}$ values into account, Figure 4b shows
528 that there is a significant along-arc variation in $\delta^{18}\text{O}$ for each mineral type, with the highest
529 plagioclase and clinopyroxene $\delta^{18}\text{O}$ values in rocks from Central Java relative to West and
530 East Java. The low values in East Java and lack of correlation between Pb isotope ratios and
531 indices of differentiation at Ijen further suggest minimal modification of magma source
532 compositions via interaction with crustal material during shallow level magmatic
533 differentiation. However, for West Java, the low $\delta^{18}\text{O}$ values may be deceptive when trying to
534 identify crustal assimilation if a low- $\delta^{18}\text{O}$ assimilant is involved. Interaction with hot ^{18}O -
535 depleted meteoric groundwater in hydrothermal circulation at the margins of the magma
536 reservoir has been suggested from $\delta^{18}\text{O}$ values and the geochemical characteristics of lavas at
537 Galunggung in West Java (Harmon and Gerbe, 1992). Salak and Guntur display $\delta^{18}\text{O}$
538 clinopyroxene values lower than the mantle range (Fig. 4c) likewise suggesting potential
539 involvement of an ^{18}O -depleted component. For Merapi, the wide range in clinopyroxene

540 $\delta^{18}\text{O}$ values (5.1 to 7.2‰), both above and below the mantle range, may indicate that both
541 ^{18}O -enriched and ^{18}O -depleted components are involved in its petrogenesis. New laser
542 fluorination O isotope mineral data for Guntur volcano also implicate the involvement of ^{18}O -
543 enriched and ^{18}O -depleted components in volcanic petrogenesis (Macpherson et al.,
544 submitted). The along-arc peak in $\delta^{18}\text{O}$ values at Central Java contrasts with the along-arc
545 peak in Pb isotope ratios, observed for West Java (Fig. 7a). However, the along-arc trend in
546 oxygen isotopes is similar to the along-arc pattern in Sr isotope composition for which there is
547 significantly more data available (Fig. 7b). This suggests that the main crustal assimilant
548 involved in West Java volcanic petrogenesis is characterised by relatively low $\delta^{18}\text{O}$ and low
549 Pb and Sr isotopic ratios. Whereas in Central Java this component may also be present but an
550 additional assimilant characterised by higher $\delta^{18}\text{O}$ values, higher Sr isotope ratio but
551 relatively conservative Pb isotope ratios, exerts significant control on the isotopic
552 composition of the erupted rocks.

553 The combined use of O and Pb isotopes can help to constrain the relative importance
554 of crustal assimilation versus subduction input of crustal material in magma genesis and
555 evolution due to the contrasting mixing trajectories that result from each process (e.g., James,
556 1981; Davidson et al., 2005). The inset diagram of Fig. 4c shows the different curvatures
557 expected for crustal assimilation (dashed lines) and subduction input of crustal material to a
558 mantle wedge source (solid lines) that arise due to the large difference in the Pb/O ratio of the
559 mantle wedge source and the mantle-derived arc magma. Mixing between the mantle source
560 and subducted crustal material results in strongly convex-downward mixing curves (Fig. 4c
561 model A and inset diagram). Whereas mixing between mantle-derived arc magma and the arc
562 crust creates largely straight or convex-upwards curves (James, 1981) (Fig. 4c model B and
563 inset diagram). Acknowledging that the exact locations of the mixing trends in Pb-O isotope
564 space are somewhat dependant on the Pb isotope ratio of the selected crustal end-member
565 (Fig. 4c inset), the Gede and other available Javanese clinopyroxene $\delta^{18}\text{O}$ data generally lie
566 along the mixing curve representing input of local subducted sediment to the mantle source
567 (Fig. 4c model A), opposed to the mixing of arc magma with local arc crust (Fig. 4c model B;
568 see figure caption for the end member composition details). The observed scatter in Gede
569 clinopyroxene $\delta^{18}\text{O}$ values, some of which are higher than the mantle $\delta^{18}\text{O}$ range, may
570 indicate the extent of modification of initial arc magma clinopyroxene $\delta^{18}\text{O}$ values by crustal
571 assimilation processes. However, this could also represent slight variations in the Pb isotopic
572 composition and/or concentration of the subducted crustal component and therefore, the

573 location of the bend in the calculated mixing curve. For Guntur and Salak, clinopyroxene
574 $\delta^{18}\text{O}$ values lower than the mantle range and below the mixing curve support some
575 involvement of an ^{18}O -depleted component in magma genesis as discussed above.
576 Nevertheless, the modelling suggests that the dominant control on O-Pb isotope systematics at
577 Gede and other West Javanese volcanoes is related to the source input of crustal material.

578

579 *6.3. Pb isotope constraints on the source components involved in magma genesis*

580 Despite evidence for some modification of initial source Pb isotope ratios via crustal
581 assimilation, the wide contrast in Pb isotope ratios of East Javanese volcanic rocks (e.g., Ijen)
582 compared to those from West and Central Java (e.g., Gede, Salak and Merbabu) at similar
583 degrees of differentiation (Fig. 4) points towards heterogeneity in the source isotope
584 composition, whether in the mantle wedge source component itself or variation in the type
585 and/or amount of the subducted input. Having established that the West Javanese volcanic
586 rocks exhibit higher Pb isotope ratios than the local crustal rocks and that the highest Pb
587 isotope ratios are observed in the least differentiated (inferred, least crustally contaminated)
588 rocks (Fig. 4), the higher Pb isotope ratios of West and Central Javanese volcanic rocks,
589 relative to East Javanese rocks, may represent a greater proportion of subducted crustal
590 material or a similar proportion of more radiogenic material in West and Central Javanese
591 rocks. Handley et al. (2011) showed that Hf-Nd isotope systematics in Javanese lavas are
592 consistent with heterogeneity in the subduction component input along the arc, largely
593 controlled by observed present-day spatial variations in the sediments deposited in the Java
594 Trench. The authors implicate the incorporation of a dominantly continental-derived, detrital-
595 rich subducted sedimentary component in the west and a more pelagic, clay-rich subducted
596 sedimentary component and possibly stronger slab-fluid imprint in the east. The significantly
597 higher radiogenic Pb isotope ratios measured in West Java volcanic rocks, relative to East
598 Java at a similar degree of magmatic differentiation (regardless of whether the highest or
599 lowest Pb isotope ratios of Gede, for example, are taken), are also consistent with a higher
600 proportion of old, detrital-rich continental material in the source in West Java. This idea is
601 explored further in Section 6.4.

602 The relatively tight Java array displayed in Pb-Pb isotope space can be utilised to
603 provide constraints on the mantle wedge source composition involved in magma genesis. The
604 Java data array projects back towards a source composition with approximately average I-
605 MORB composition ($n = 43$, Fig. 3a and b) with little or no requirement for an Indian Ocean
606 seamount-source component (I-Seamount East; Fig. 3b). The tight, linear array suggests a

607 relatively homogenous mantle source composition for the Javanese volcanoes presented. This
608 contrasts with the suggestion by Handley et al. (2007) that there may be potential
609 heterogeneity in this component. Handley et al. (2007) implicated a mantle source
610 composition with lower than average $^{176}\text{Hf}/^{177}\text{Hf}$ for Ijen (and by inference East Java) relative
611 to Central and West Java. However, an average I-MORB source Pb isotopic composition is
612 sufficient to explain the overall Java Pb isotope data.

613 On a Pb-Pb isotope diagram, simple mixing between two components will produce a
614 straight line. The new and previously published data for Javanese volcanoes (excluding
615 Merapi volcano) appear to lie on a simple binary mixing line between average I-MORB,
616 representing the mantle source, and bulk Indian Ocean sediment (I-SED) exemplified by the
617 mixing line between I-MORB and the bulk Java subducted sediment composition of Plank
618 and Langmuir (1998) shown in Figures 3a and b. However, several of the local upper crust
619 rocks, represented by Sumatran intrusive rocks and sedimentary rocks from Central Java,
620 overlap with the field for I-SED. Therefore, from the Pb-Pb diagram alone, the exact nature of
621 the crustal component involved during petrogenesis is not discernable.

622 It is more difficult to determine the role of a slab fluid produced by dehydration of the
623 down-going altered oceanic crust (AOC) from Pb isotopes. Hydrothermal alteration processes
624 at the ridge-crest may result in a significant amount of Pb being extracted from the oceanic
625 crust prior to subduction (e.g., Albarède and Michard, 1989) minimising the imprint of any
626 addition of this component to the mantle source. However, an estimate of the Pb isotopic
627 composition of an AOC liberated fluid can be gained by using the compositions of Indian
628 Ocean ferromanganese crusts (Mn nodules) (O’Nions et al., 1998; Frank and O’Nions, 1998).
629 Manganese nodules scavenge and incorporate trace metals from seawater and hence record
630 the isotopic composition of ambient seawater (e.g., Goldstein and O’Nions, 1981; Albarède
631 and Goldstein, 1992; Frank and O’Nions, 1998) that would have interacted with I-MORB.
632 Therefore, the Pb isotopic composition of the AOC fluid component is likely to lie on a
633 mixing line between I-MORB and the composition of Mn nodules in Pb-Pb isotope space. As
634 can be seen from Figures 3a and b, the field for 0-20 Ma old Indian Ocean Mn nodules
635 overlaps almost completely with the I-SED field and several upper crust sedimentary rocks
636 and, therefore, this component cannot from its Pb isotope composition alone be distinguished
637 from subducted sediment input or crustal assimilation. The involvement of an AOC
638 component will be discussed further in Section 6.4 using a combined Pb isotope-trace element
639 ratio approach. The Pb isotope composition of the altered oceanic crust end-member used in
640 modelling Sunda and Banda arc volcanic petrogenesis by Edwards et al. (1993) lies at a

641 reasonable position in $^{208}\text{Pb}/^{204}\text{Pb}$ - $^{206}\text{Pb}/^{204}\text{Pb}$ space (Fig. 3b). However, the proposed
642 $^{207}\text{Pb}/^{204}\text{Pb}$ composition of this component appears to be significantly low, lying on the
643 northern hemisphere reference line (NHRL; Hart, 1984) and not on a mixing line between I-
644 MORB and the Mn crusts. This is probably due to the fact that Edwards et al. (1993) used a
645 generic estimated AOC composition and did not use local end-member (Indian Ocean)
646 compositions, presumably due to the lack of published altered Indian MORB data. We
647 suggest that their $^{207}\text{Pb}/^{204}\text{Pb}$ ratio is unlikely to be representative of the true $^{207}\text{Pb}/^{204}\text{Pb}$ ratio
648 of AOC fluid at the Sunda arc.

649

650 *6.4. Combined Pb isotopic and trace element constraints on subduction input variability*

651 Barium concentrations in Javanese volcanic rocks show considerable variation along the
652 island, with East and Central Java (excluding Slamet) displaying significantly higher
653 concentrations than those in West Java for a given SiO_2 content (Fig. 8a). Despite some
654 scatter in individual volcanic suites for Central and East Java, the differentiation trends for the
655 geographic suites form largely parallel, positive arrays (noting the exceptionally high Ba
656 concentrations of some Lamongan and Tengger Caldera volcanic rocks) that do not converge
657 upon a common parental composition when projected backwards to less evolved SiO_2
658 contents. This suggests that the differences in Ba concentrations of the Javanese rocks result
659 from heterogeneity in the source region rather than from shallow-level assimilation processes
660 during magmatic evolution.

661 Barium, as a large ion lithophile element (LILE), is considered highly mobile in
662 subduction-related fluids relative to the more fluid-immobile, light rare earth elements
663 (LREE) and the high field strength element (HFSE) Hf (Hawkesworth et al, 1993; Keppler,
664 1996; Kogiso et al., 1997; Kessel et al., 2005). Therefore, Ba/Hf ratios combined with the Pb
665 isotope compositions of the Javanese volcanic rocks may yield potential insight into
666 variations in subduction-related components along the island. Higher Ba/HFSE (e.g., Ba/Hf,
667 Ba/Nb) and Ba/LREE (e.g., Ba/La) ratios in arc lavas, relative to depleted upper mantle
668 values, are usually attributed to significant input of an altered oceanic crust fluid component
669 (e.g., Elliott et al., 1997; Woodhead et al., 2001) but equally may result from the contribution
670 of hydrous melts of subducted sediment (e.g., Kelemen et al., 2003; Hermann and Rubatto,
671 2009; Jicha et al., 2010). High Ba concentrations, up to 3500 ppm, are reported in drilled
672 Indian Ocean sediments (Gasparon and Varne, 1998). Figure 8b highlights the clear
673 geographic differences of volcanic rocks in West (~high Pb isotope ratios and relatively low
674 Ba/Hf), Central (moderately high Pb isotope ratios and high Ba/Hf) and East (relatively low

675 Pb isotope ratios and moderate to high Ba/Hf) Java. The boxed arrows on Figure 8b show the
676 estimated maximum modification of Gede source Ba/Hf and Pb isotope ratios due to crustal
677 assimilation. We anticipate a relatively similar, or smaller impact from crustal assimilation on
678 the source Ba/Hf ratios and Pb isotopes of the Central Javanese rocks (Merapi and Merbabu)
679 due to 1) their more restricted range in Pb isotope ratio, 2) the low Ba/Hf ratios and low Pb
680 isotopic ratios of local carbonaceous sedimentary rocks (e.g., Table 3; Fig. 5) and 3) that
681 Slamet volcano, which also displays similarly high Sr isotope ratios compared to the other
682 Central Javanese volcanoes, has low Ba/Hf ratios similar to the West Javanese volcanic rocks
683 (Fig. 7). Nonetheless, regardless of whether the highest or lowest Pb isotope ratio for Gede or
684 Merapi/Merbabu is taken as the rock least affected by crustal assimilation, the geochemical
685 contrasts between the geographic regions still remain.

686 Simple bulk-mixing models between an I-MORB source and Indian Ocean sediment
687 end-members (see Fig. 8 caption for details) show that the differences in isotopic and trace
688 element ratios between West and East Java can be explained via heterogeneity in the
689 subducted sediment contribution, largely reflecting present-day spatial variations in sediment
690 compositions on the down-going plate in the Java Trench. A low or high Ba/Hf and higher Pb
691 isotopic composition (e.g., detrital-rich) sediment is required for West Java versus a high
692 Ba/Hf, low Pb isotopic composition (e.g., pelagic, clay-rich) sediment is required for East
693 Java. This suggestion of heterogeneity in the subducted sediment component along Java is
694 similar to that proposed by Handley et al. (2011) using Nd-Hf isotopic compositions of
695 Javanese volcanic rocks. If sediment melts/fluids are involved, rather than bulk-sediment
696 addition, the subducted sediment percentage contributions required are smaller than those
697 shown in Figure 8.

698 An alternative hypothesis to the involvement of a heterogeneous subducted
699 sedimentary component is assimilation of a heterogeneous sedimentary component in the
700 crust. Clements et al. (2009) suggested that the Late Eocene to Early Miocene basin-filling
701 sediment composition varies along Java: West and Central Java basins were supplied with
702 quartz-rich clastic sediments by rivers draining the Sunda Shelf whereas East Java was largely
703 supplied by Eocene to Miocene volcanoclastic products of the Southern Mountains Arc.
704 Crustal assimilation of old, continentally-derived sediments, presumably with radiogenic Pb
705 isotope compositions in West Java, relative to East Java, may explain the eastward decrease in
706 Pb isotope ratios along the island. However, the low, mantle-like $\delta^{18}\text{O}$ values of mineral
707 separates from West Java volcanic rocks would require relatively deep assimilation of the
708 basin-fill sediments, prior to significant magmatic differentiation to avoid 1) O-isotope

709 modification of the assimilant by low-temperature meteoric fluid, and 2) the detection of
710 assimilation of this component utilising radiogenic isotope and SiO₂ variations. Therefore, we
711 prefer a model of subducted sediment involvement to explain the contrasts in Pb isotope
712 ratios along Java. Furthermore, the addition of arc crust to a magma has less leverage on the
713 Pb concentration (and thereby Pb isotope ratio) than addition of subducted crustal
714 components to the mantle wedge source, due to the significantly low concentration of Pb of
715 the mantle wedge. Therefore, the impact of crustal assimilation will likely be less than the
716 impact of source input of crustal material upon the resultant Pb isotope ratios. This conclusion
717 is consistent with a recent study on the chemical and isotopic (He-C-N) characterisation of
718 active fumaroles and hydrothermal gases and waters from the summits and flanks of multiple
719 volcanic centres along the western Sunda arc (Halldórsson et al., 2013), which suggested that
720 subduction-related source contamination plays the dominant role over thick/old crustal
721 basement in supplying the major volatile output budget of the western Sunda arc volcanoes.

722 The higher Ba/Hf ratios in East Javanese and possibly also Central Javanese rocks
723 may be attributed to either greater contribution of high-Ba/Hf sediment (fluid/melt) and/or the
724 more significant involvement of an AOC fluid component compared to West Java. A melt
725 inclusion study of Ijen and Tambora volcanic rocks (Vigouroux et al., 2012) suggested that
726 Ijen records a higher AOC-derived fluid component relative to Galunggung and Tambora,
727 with AOC being the main source of Sr and volatiles and subducted sediment melt being an
728 important component for Ba, Pb, Th and the LREE. Although we note that Vigouroux et al.
729 (2012) did not take into consideration the impact of crustal assimilation in their study. An
730 AOC and/or Roo Rise (I-Seamount East) lithospheric liberated fluid component is likely to
731 have less radiogenic Pb isotope compositions than the Javanese volcanic rocks (Section 6.3,
732 Fig. 3) and, therefore, mixing alone between I-MORB and AOC or subducted lithospheric
733 fluid is not sufficient to explain the volcanic data. However, we propose that subduction of
734 the Roo Rise south of Central and East Java (~109°E to 115°E at the trench, ~110°E to 116°E
735 beneath Java; Fig. 1) has a significant impact upon the subduction component in Java and
736 hence the geochemical and isotopic composition of the erupted volcanic rocks. The peak in
737 Ba/Hf and Ba/Nb at Kelut and Tengger Caldera (~112-113°E) (Fig. 7c and inset) corresponds
738 to the centre of the region affected by collision of the Roo Rise (Figs. 1 and 2), and Ba/Hf
739 (and Ba/Nb) decreases relatively systematically at volcanoes either side of this location. The
740 bathymetric survey by Kopp et al. (2006) shows that the outer rise region of the Indian Ocean
741 plate south of Central and East Java is extensively fractured (trench-parallel normal faults)
742 compared to West Java, related to plate bending induced tectonic stress. The faulting and

743 associated morphological effects caused by subduction of the Roo Rise will increase surface
744 roughness and, therefore, the surface area available for interaction of the subducted
745 lithosphere with seawater (e.g., Ranero et al., 2003). The higher fluid-mobile/non-fluid
746 mobile ratios in East Javanese volcanic rocks may reflect the enhanced water content of the
747 heavily fractured, down-going altered and/or serpentinised oceanic lithosphere in this region.
748 Enhanced fluid addition and, therefore, fluid-fluxing to the mantle wedge may be expected to
749 result in higher degrees of partial melting of the mantle source. However, the general lack of
750 correlation between Ba/Hf and indicators of the degree of mantle melting (e.g., La/Yb; Fig. 9)
751 in East and Central Javanese volcanic rocks (excluding Ungaran), which show a wide range in
752 Ba/Hf at relatively constant La/Yb, is inconsistent with a systematic increase in fluid-flux
753 melting towards Kelut from the East (Ijen) and West (~Slamet). We do note though that Kelut
754 volcanic rocks have the highest Ba/Hf and amongst the lowest La/Yb ratios of Javanese
755 volcanic rocks, indicative of the greatest degrees of partial melting of the source as might be
756 expected at the centre of the collision-affected region. In contrast, strong correlations between
757 concentrations of fluid-mobile elements (e.g., B), B/La, B/Be and Sr isotope ratios and
758 degrees of mantle melting (La/Yb) have been observed at the Aleutian arc and attributed to
759 subduction of the Amila Fracture Zone in the central Aleutian arc (Singer et al., 1996).
760 Subduction of the fracture zone is proposed to have channelled large quantities of sediment
761 and water into the subarc mantle (Singer et al., 1996). Despite the low La/Yb observed in
762 rocks from Kelut, the overall limited correlation in Javanese rocks of Ba/Hf with La/Yb
763 suggests that the addition of expelled fluid may take place at relatively shallow depth, or there
764 is a greater involvement of high Ba concentration, subducted sedimentary material in volcanic
765 petrogenesis in East and possibly Central Java, relative to West Java. The generally low
766 initial concentration of Ba in serpentinite and experimental serpentinite fluid/residue partition
767 coefficients, led Tenthorey and Hermann (2004) to conclude that Ba enrichment in arc lavas
768 must be largely derived from the subducted sediments. However, the increased fluid-flux
769 available from the heavily-fractured Roo Rise lithosphere likely enables larger degrees of
770 melting of the subducted sediments and scavenging of LILE from the altered oceanic crust
771 (e.g., Ranero et al., 2003). The degree of subducted lithospheric bend faulting, and the
772 incoming plate composition have been linked to the regional trends in lava chemistry for
773 Central American arc volcanism (Rüpke et al., 2002). The transition from subduction
774 accretion (west of ~109°E at the Java Trench) to subduction erosion (east of ~109°E at the
775 Java Trench) (Kopp et al., 2006) may also play a role in providing additional high-Ba pelagic
776 sediments (that were formally part of the accretionary wedge) to the arc element-recycling

777 budget in East Java. Several studies have suggested that the global subduction erosion flux
778 may be significantly larger than the global subducted sediment flux (e.g., von Huene and
779 Scholl, 1991; Clift et al., 2009; Scholl and von Huene, 2009).

780

781 **7. Conclusions**

782 New Pb isotope data for Javanese volcanoes and local upper crust, in conjunction with O
783 isotope and geochemical data, have provided new insight into the relative importance of
784 crustal assimilation versus subducted crustal input in Javanese volcanic petrogenesis. Despite
785 varying degrees of modification of geochemical and isotope data by crustal assimilation
786 processes, heterogeneity in the subducted input (fluid and/or sediment melt) is required to
787 explain the significant geochemical and isotopic contrasts observed between West and East
788 Java (e.g., Ba concentration, Ba/Hf ratio and Pb isotopic composition).

789 We identify two crustal assimilants in West and Central Java: 1) a low $\delta^{18}\text{O}$ and
790 relatively low Pb and Sr isotopic composition assimilant in West Java (at Gede Volcanic
791 Complex), likely representing more primitive arc rocks or mafic-ultramafic ophiolitic rocks,
792 known to outcrop in West (and Central) Java and 2) a higher $\delta^{18}\text{O}$, higher Sr isotope
793 composition assimilant in Central Java, which is consistent with the proposed assimilation of
794 crustal carbonate material for Merapi in Central Java (Chadwick et al., 2007; Deegan et al.
795 2010; Troll et al., 2013), providing that the carbonate assimilant is characterised by a
796 relatively unradiogenic to moderately radiogenic Pb isotopic composition and low Ba/Hf.
797 However, assimilation of carbonate material in Central Java cannot exert much control the
798 geochemical composition of the erupted rocks in comparison to Vesuvius volcano, where the
799 dominance of carbonate assimilation is clearly documented and manifest in the negative
800 correlation of $\text{Na}_2\text{O}+\text{K}_2\text{O}$ with SiO_2 (Iacono Marziano et al., 2008). Positive correlations
801 between $\text{Na}_2\text{O}+\text{K}_2\text{O}$ with SiO_2 are observed in the majority of Javanese volcanic rocks. The
802 East Javanese volcanic rocks provide little evidence for isotopic modification via crustal
803 assimilation. We suggest that this is due to significant transitions in the crustal architecture
804 and composition between West and Central and Eastern Java at the Central Java Fault/Progo-
805 Muria lineament.

806 After consideration of the geochemical and isotopic effects of crustal assimilation, the
807 remaining significant heterogeneity observed in East and West Java volcanic rock Ba
808 concentrations, Ba/Hf ratios and Pb isotopic compositions is likely attributed to heterogeneity
809 in the subduction input source component. The high Ba/Hf and lower Pb isotope ratios in East
810 Javanese relative to West Javanese rocks implicate a higher fluid-component and/or greater

811 incorporation of high Ba/Hf detrital-poor (clay-rich) pelagic sediments in East Java relative to
812 West Java. The collision of the Roo Rise with the Java margin between 109°E and 115°E may
813 provide additional fluid-flux (and greater scavenging of fluid mobile elements) and increased
814 melting of sediment. The transition from subduction accretion to subduction erosion from
815 West to East Java may also play an important role in increasing the budget of crustal material
816 available for subduction recycling in East Java. The tight Javanese Pb isotope array projects
817 back towards a composition consistent with an average I-MORB source.

818 We note for future studies that: 1) if limestone/carbonaceous sediment assimilation is
819 significant, the ‘least evolved rocks’ of a volcanic suite may not represent the least
820 ‘contaminated’ magma, and 2) where there is a wide variation in isotopic ratios over a limited
821 range in SiO₂ or MgO contents, along-arc studies selecting just one or two basaltic samples to
822 characterise an entire volcano may not accurately represent the most mantle source-like
823 composition. We stress that only through detailed studies of individual volcanoes, prior to
824 along-arc syntheses, will it be possible to fully constrain the relative roles of different crustal
825 inputs in arc settings.

826

827 **8. Acknowledgements**

828 We are thankful to Jon Davidson for the discussion of early ideas behind this manuscript.
829 Juan Carlos Afonso is thanked for producing the Digital Elevation Model maps from SRTM
830 data. Sample collection was assisted by a NERC studentship (NER/S/A/2001/06127) and the
831 South East Asia Research Group (SEARG) at Royal Holloway University of London.
832 Galunggung samples were provided to ST by Steve Weaver and Sutikno Bronto. We thank
833 Anders Meibom for the editorial handling of the manuscript and two anonymous reviewers
834 for their helpful suggestions and comments. HH acknowledges support from an Australian
835 Research Council Future Fellowship FT120100440 and JBT acknowledges support from the
836 French Agence Nationale de la Recherche through the grant ANR-10-BLANC-0603 M&Ms –
837 Mantle Melting – Measurements, Models, Mechanisms. Merbabu isotope analyses were
838 supported by a German Research Foundation (DFG) Grant Ke 136/31.

839

840 **References**

841 Abdurrachman A. (2012). Geology and petrology of Quaternary Papandayan volcano and
842 genetic relationship of volcanic rocks from the Triangular Volcanic Complex around
843 Bandung Basin, West Java, Indonesia. Ph.D. Thesis, Akita University, Japan.

844 Abdurrachman, M., Yamamoto, M. (2012). Geochemical variation of Quaternary volcanic
845 rocks in Papandayan area, West Java, Indonesia: A role of crustal component. *Journal*
846 *of the Geological Society of Thailand, GEOSEA2012*, 40-57.

847 Albarède F. and Goldstein S. L. (1992). World map of Nd isotopes in seafloor
848 ferromanganese deposits. *Geology* 20, 761–763.

849 Albarède F. and Michard, A. (1989). Hydrothermal alteration of the oceanic crust. In:
850 *Crust/mantle recycling at convergence zones*. Eds Hart, S.R. and Gülen, L. p29-37
851 (Kluwer Academic Publishers, Dordrecht, The Netherlands).

852 Anderson, A.T. (1976). Magma mixing: petrological process and volcanological tool. *J. Volc.*
853 *Geotherm. Res.* 1, 3-33.

854 Ben Othman, D.B., White, W.M., Patchett, J. (1989). The geochemistry of marine sediments,
855 island arc magma genesis, and crust-mantle recycling. *Earth Planet. Sci. Lett.*, 94: 1-21.

856 Bindeman, I.N., Fournelle, J.H., Valley, J.W. (2001). Low- $\delta^{18}\text{O}$ tephra from a
857 compositionally zoned magma body: Fisher Caldera, Unimak Island, Aleutians. *J. Volc.*
858 *Geotherm. Res.* 111, 35-53.

859 Camus, G., Gourgaud, A., Vincent, P.M. (1987). Petrological evolution of Krakatau
860 (Indonesia): Implications for a future activity. *J. Volc. Geother. Res.* 33, 299-316.

861 Carn, S.A., Pyle, D.M. (2001). Petrology and geochemistry of the Lamongan Volcanic Field,
862 East Java, Indonesia: Primitive Sunda Arc magmas in an extensional tectonic setting? *J.*
863 *Petrol.* 42, 1643-1683.

864 Carpentier, M., Chauvel, C., Mattielli, N. (2008). Pb–Nd isotopic constraints on sedimentary
865 input into the Lesser Antilles arc system. *Earth Planet. Sci. Lett.* 272, 199–211.

866 Chadwick, J.P., Troll, V.R., Ginibre, C., Morgan, D., Gertisser, R., Waight, T.E., Davidson,
867 J.P. (2007). Carbonate assimilation at Merapi Volcano, Java, Indonesia: insights from
868 crystal isotope stratigraphy. *J. Petrol.* 48, 1793–1812.

869 Chauvel, C., Blichert-Toft, J. (2001). A hafnium isotope and trace element perspective on
870 melting of the depleted mantle. *Earth Planet. Sci. Lett.*, 190: 137-151.

871 Chotin, P., Rasplus, L., Rampnoux, J.P., Suminta, Nur Hasim (1984). Major strike slip fault
872 zone and associated sedimentation in the central part of Java island (Indonesia) (in
873 French). *Bull. Soc. Geol. France* 6, 1259–1268.

874 Claproth, R. (1989). Petrography and geochemistry of volcanic rocks from Ungaran, Central
875 Java, Indonesia. Ph.D. Thesis, University of Wollongong, Australia.

876 Clements, B., Hall, R., Smyth, H.R., Cottam, M.A. (2009). Thrusting of a volcanic arc: a new
877 structural model for Java. *Petrol. Geosci.* 15, 159–174.

878 Clements, B., Hall, R. (2007). Cretaceous to Late Miocene stratigraphic and tectonic
879 evolution of West Java. Proceedings, Indonesian Petroleum Association, Thirty-First
880 Annual Convention and Exhibition, May 2007.

881 Clift, P.D., Vannucchi, P., Morgan, J.P. (2009). Crustal redistribution, crust-mantle recycling
882 and Phanerozoic evolution of the continental crust. *Earth-Science Reviews* 97, 80–104.

883 Davidson, J.P. (1987). Crustal contamination versus subduction zone enrichment: Examples
884 from the Lesser Antilles and implications for mantle source compositions of island arc
885 volcanic rocks. *Geochim. Cosmochim. Acta*, 51: 2185-2198.

886 Davidson, J.P., Dungan, M.A., Ferguson, K.M., Colucci, M.T. (1987). Crust-magma
887 interactions and the evolution of arc magmas: The San Pedro Pellado volcanic complex,
888 southern Chilean Andes. *Geology*, 15: 443-446.

889 Davidson, J.P., Harmon, R.S. (1989). Oxygen isotope constraints on the petrogenesis of
890 volcanic arc magmas from Martinique, Lesser Antilles. *Earth Planet. Sci. Lett.*, 95: 255-
891 270.

892 Davidson, J.P., Hora, J.M., Garrison, J.M., Dungan, M.A. (2005) Crustal forensics in arc
893 magmas. *J. Volcanol. Geotherm. Res.* 140, 157–170.

894 Deegan, F.M., Troll, V.R., Freda, C., Misiti, V., Chadwick, J.P., McLeod, C.L., Davidson,
895 J.P. (2010). Magma–carbonate interaction processes and associated CO₂ release at
896 Merapi Volcano, Indonesia: insights from experimental petrology. *Journal of Petrology*
897 51, 1027–1051.

898 DeMets, C., Gordon, R.G., Argus, D.F., Stein, S. (1990). Current plate motions. *Geophysical*
899 *Journal International*, 101(2): 425-478.

900 DePaolo, D.J. (1981). Trace element and isotopic effects of combined wallrock assimilation
901 and fractional crystallization. *Earth Planet. Sci. Lett.* 53, 189–202.

902 Edwards, C.M.H. (1990). Petrogenesis of tholeiitic, calc-alkaline and alkaline volcanic rocks,
903 Sunda arc, Indonesia. Ph.D. Thesis, Royal Holloway, University of London, UK.

904 Edwards, C. M. H., Morris, J. D. & Thirlwall, M. F. (1993). Separating mantle from slab
905 signatures in arc lavas using B/Be and radiogenic isotope systematics. *Nature* 362, 530-
906 533.

907 Eiler, J.M. (2001). Oxygen isotope variations of basaltic lavas and upper mantle rocks.
908 *Reviews in Mineralogy and Geochemistry*. No. 43. Mineralogical Society of America,
909 Washington, DC, pp. 319-364

- 910 Eisele, J., Abouchami, W., Galer, S.J.G., Hofmann, A.W. (1993). The 320 kyr Pb isotope
911 evolution of Mauna Kea lavas recorded in the HSDP-2 drill core. *Geochem. Geophys.*
912 *Geosyst.*, 4(5), 8710, doi:10.1029/2002GC000339.
- 913 Elliott, T., Plank, T., Zindler, A., White, W., Bourdon, B. (1997). Element transport from slab
914 to volcanic front in the Mariana arc. *Journal of Geophysical Research* 102 (B7), 14991–
915 15019.
- 916 Frank, M., O’Nions, R.K. (1998). Sources of Pb for Indian Ocean ferromanganese crusts: a
917 record of Himalayan erosion? *Earth and Planetary Science Letters* 158, 121–130.
- 918 Gao, Y., Hoefs, J., Przybilla, R., Snow, J. E. (2006). A complete oxygen isotope profile
919 through the lower oceanic crust, ODP Hole 735B. *Chemical Geology* 233, 217–234.
- 920 Garwin, S., Hall, R., Watanabe, Y. (2005). Tectonic setting, geology and gold and copper
921 mineralization in Cenozoic magmatic arcs of Southeast Asia and the west Pacific. In:
922 Hedenquist J, Goldfarb R, Thompson J (eds) *Economic geology 100th anniversary*
923 *volume, Soc Econ Geol*, pp 891–930
- 924 Gasparon, M., Varne, R. (1995). Sumatran granitoids and their relationship to Southeast
925 Asian terranes. *Tectonophysics* 251, 277–299.
- 926 Gasparon, M., Varne, R. (1998). Crustal assimilation versus subducted sediment input in west
927 Sunda arc volcanics: an evaluation. *Mineral. Petrol.* 64, 89–117.
- 928 Gerbe, M.-C., Gouraud, A., Sigmarsson, O., Harmon, R.S., Joron, J-L., Provost, A. (1992).
929 Mineralogical and geochemical evolution of the 1982-1983 Galunggung eruption
930 (Indonesia). *Bulletin of Volcanology*, 54: 284-298.
- 931 Gertisser, R., Keller, J. (2003a). Trace element and Sr, Nd, Pb and O isotope variations in
932 medium-K and high-K volcanic rocks from Merapi Volcano, Central Java, Indonesia:
933 evidence for the involvement of subducted sediments in Sunda Arc magma genesis. *J.*
934 *Petrol.* 44, 457–489.
- 935 Gertisser, R., Keller, J. (2003b). Temporal variations in magma composition at Merapi
936 Volcano (Central Java, Indonesia): magmatic cycles during the past 2000 years of
937 explosive activity. *J. Volc. Geotherm. Res.* 123, 1–23.
- 938 Goldstein S. L. and O’Nions R. K. (1981). Nd and Sr isotopic relationships in pelagic clays
939 and ferromanganese deposits. *Nature* 292, 324–327.
- 940 Hall, R. (2002). Cenozoic geological and plate tectonic evolution of SE Asia and the SW
941 Pacific: computer-based reconstructions, model and animations. *J Asian Earth Sci.* 20,
942 353-431.

943 Hall, R. (2011). Australia-SE Asia collision: plate tectonics and crustal flow. Geological
944 Society, London, Special Publications 355, 75-109..

945 Halldórsson, S.A., Hilton, D.R., Troll, V.R., Fischer, T.P. (2013). Resolving volatile sources
946 along the Western Sunda arc, Indonesia. *Chemical Geology* 339, 263-282.

947 Hamilton, W.B. (1979). Tectonics of the Indonesian region. U.S. Geological Survey
948 Professional Paper reprinted with corrections, 1981 and 1985, 1078: 345.

949 Handley, H.K. (2006). Geochemical and Sr-Nd-Hf-O isotopic constraints on volcanic
950 petrogenesis at the Sunda arc, Indonesia, PhD Thesis, Durham University, UK.
951 <http://etheses.dur.ac.uk/2670/>

952 Handley, H.K., Macpherson, C.G., Davidson, J.P., Berlo, K., Lowry, D. (2007). Constraining
953 fluid and sediment contributions to subduction-related magmatism in Indonesia: Ijen
954 Volcanic Complex, Indonesia. *J. Petrol.* 48, 1155–1183.

955 Handley, H.K., Davidson, J.P., Macpherson, C.G. (2008a). Untangling differentiation in arc
956 lavas: constraints from unusual minor and trace element variations at Salak Volcano,
957 Indonesia. *Chem. Geol.* 255, 360–376.

958 Handley H.K., Turner S., Smith I.E.M., Stewart R.B., Cronin S.J. (2008b). Rapid timescales
959 of differentiation and evidence for crustal contamination at intra-oceanic arcs:
960 geochemical and U–Th–Ra–Sr–Nd isotopic constraints from Lopevi Volcano, Vanuatu,
961 SW Pacific. *Earth Planet Sci Lett* 273:184–194.

962 Handley, H.K., Macpherson, C.G., Davidson, J.P. (2010). Geochemical and Sr–O isotopic
963 constraints on magmatic differentiation at Gede Volcanic Complex, West Java,
964 Indonesia. *Contrib. Mineral. Petrol.* 159, 885–908.

965 Handley, H.K., Turner, S., Macpherson, C.G., Gertisser, R., Davidson, J.P. (2011). Hf–Nd
966 isotope and trace element constraints on subduction inputs at island arcs: Limitations of
967 Hf anomalies as sediment input indicators. *Earth Planet. Sci. Lett.* 304 212–223.

968 Harmon, R.S., Gerbe, M-C. (1992). The 1982-83 Eruption at Galunggung Volcano, Java
969 (Indonesia): Oxygen Isotope Geochemistry of a Chemically Zoned Magma Chamber.
970 *Journal of Petrology* 33, 585-609.

971 Harmon, R.S., Hoefs, J. (1995). Oxygen isotope heterogeneity of the mantle deduced from
972 global ¹⁸O systematics of basalts from different geotectonic settings. *Contrib Mineral*
973 *Petrol* 120, 95-114.

974 Hart, S. R. (1984). A large-scale isotope anomaly in the Southern Hemisphere mantle. *Nature*
975 309, 753-757.

- 976 Hartono, U. (1996). Stratigraphic geochemical trends of the Wilis Volcanic Complex, Eastern
977 Sunda Arc: Implication for the magma evolution. *GRDC Bulletin*, 19, 97-133.
- 978 Hawkesworth, C.J., Hergt, J.M., Ellam, R.M., McDermott, F. (1991). Element fluxes
979 associated with subduction related magmatism. *Philos. Trans. R. Soc. Lond. A.*, 335:
980 393-405.
- 981 Hawkesworth, C.J., Gallagher, K., Hergt, J.M., McDermott, F. (1993). Mantle and slab
982 contributions in arc magmas. *Annual Review of Earth and Planetary Sciences* 21, 175–
983 204.
- 984 Hegner, E., Roddick, J.C., Fortier, S.M., Hulbert, L. (1995a). Nd, Sr, Pb, Ar and O isotopic
985 systematics of Sturgeon Lake kimberlite, Saskatchewan, Canada: constraints on
986 emplacement age, alteration, and source composition. *Contrib. Mineral. Petrol.*, 120,
987 212-222.
- 988 Hegner, E., Walter, H.J., Satir, M. (1995b). Pb-Sr-Nd isotopic compositions and trace element
989 geochemistry of megacrysts and melilitites from the Tertiary Urach volcanic field:
990 source composition of small volume melts under SW Germany. *Contrib. Mineral.
991 Petrol.* 122, 322-335.
- 992 Hermann, J., Rubatto, D. (2009). Accessory phase control on the trace element signature of
993 sediment melts in subduction zones, *Chem. Geol.*, 265(3–4), 512–526,
994 doi:10.1016/j.chemgeo.2009.05.018.
- 995 Hildreth, W., Moorbath, S. (1988). Crustal contributions to arc magmatism in the Andes of
996 Central Chile. *Contrib. Mineral. Petrol.*, 98: 455-489.
- 997 Hoffmann-Rothe, A., Ritter, O., Haak, V. (2001). Magnetotelluric and geomagnetic
998 modelling reveals zones of very high electrical conductivity in the upper crust of
999 Central Java. *Physics of The Earth and Planetary Interiors*, 124(3-4): 131-151.
- 1000 Hoernle, K. Hauff, F., Werner, R., van den Bogaard, P., Gibbons, A. D., Conrad S., Muller,
1001 R.D. (2011). Origin of Indian Ocean Seamount Province by shallow recycling of
1002 continental lithosphere. *Nature Geoscience* 4, 883-887.
- 1003 Huppert, H.E., Sparks, R.S.J. (1985). Cooling and contamination of mafic and ultramafic
1004 magmas during ascent through continental crust. *Earth Planet. Sci. Lett.* 74, 371-386.
- 1005 Hutchison, C.S. (1975). Ophiolite in Southeast Asia. *Geological Society of America Bulletin*
1006 86, 797-806.
- 1007 Hutchison, C.S. (1976). Indonesian active volcanic arc: K, Sr and Rb variation with depth to
1008 the Benioff zone. *Geology*, 4: 407-408.

- 1009 Hutchison, C.S. (1982). Indonesia. Andesites: Orogenic Andesites and Related Rocks: 207-
1010 224.
- 1011 Iacono Marziano, G., Gaillard, F., Pichavant, M. (2008). Limestone assimilation by basaltic
1012 magmas: an experimental re-assessment and application to Italian volcanoes. *Contrib.*
1013 *Mineral. Petrol.* 155:719–738 doi: 10.1007/s00410-007-0267-8.
- 1014 Ito, E., Stern, R.J. (1986). Oxygen- and strontium-isotopic investigations of subduction zone
1015 volcanism: the case of the Volcano Arc and the Marianas Island Arc. *Earth Planet. Sci.*
1016 *Lett.* 76, 312-320.
- 1017 Ito, E., White, W.M., Gopel, C. (1987). The O, Sr, Nd and Pb isotope geochemistry of
1018 MORB. *Chemical Geology*, 62: 157-176.
- 1019 James, D.E. (1981). The combined use of oxygen and radiogenic isotopes as indicators of
1020 crustal contamination. *Ann. Rev. Earth. Planet. Sci.* 9, 311-44.
- 1021 James, D.E. (1982). A combined O, Sr, Nd, and Pb isotopic and trace element study of crustal
1022 contamination in central Andean lavas, I. Local geochemical variations. *Earth Planet.*
1023 *Sci. Lett.* 57, 47-62 .
- 1024 Jeffery A. J., Gertisser R., Troll V. R., Jolis E. M., Dahren B., Harris C., Tindle A. G., Preece
1025 K., O'Driscoll B., Humaida H., Chadwick J. P. (2013). The pre-eruptive magma
1026 plumbing system of the 2007–2008 dome-forming eruption of Kelut volcano, East Java,
1027 Indonesia. *Contrib Mineral Petrol* 166, 275-308. doi 10.1007/s00410-013-0875-4
- 1028 Jicha, B. R., Smith, K. E., Singer, B. S., Beard, B. L., Johnson, C. M., Rogers, N. W. (2010).
1029 Crustal assimilation no match for slab fluids beneath Volcán de Santa María,
1030 Guatemala. *Geology*, 38, 859-862; doi: 10.1130/G31062.1
- 1031 Kadarusman, A., Massonne, H.-J., van Roermund, H., Permana, H., Munasri (2007). P-T
1032 Evolution of Eclogites and Blueschists from the Luk Ulo Complex of Central Java,
1033 Indonesia, *International Geology Review*, 49:4, 329-356; doi.org/10.2747/0020-
1034 6814.49.4.329
- 1035 Kelemen, P.B., Yogodzinski, G.M., Scholl, D.W. (2003). Along strike variation in lavas of
1036 the Aleutian islandarc: genesis of highMg#andesite and implications for continental
1037 crust. In: Eiler, J. (Ed.), *Inside the Subduction Factory*, 138. AGU Monograph, pp. 223–
1038 276.
- 1039 Keppler, H. (1996). Constraints from partitioning experiments on the composition of
1040 subduction zone fluids. *Nature*, 380: 237-240.

- 1041 Kessel, R., Schmidt, M.W., Ulmer, P., Pettker, T. (2005). Trace element signature of
 1042 subduction-zone fluids, melts and supercritical liquids at 120-180 km depth. *Nature*,
 1043 437: 724-727.
- 1044 Kogiso, T., Tatsumi, Y., Nakano, S. (1997). Trace element transport during dehydration
 1045 processes in the subducted oceanic crust: 1. Experiments and implications for the origin
 1046 of ocean island basalts. *Earth and Planetary Science Letters* 148, 193-205.
- 1047 Kopp, H., Flueh, E.R., Petersen, C.J. Weinrebe, W. Wittwer, A. Meramex Scientists. (2006).
 1048 The Java margin revisited: Evidence for subduction erosion off Java. *Earth and*
 1049 *Planetary Science Letters* 242, 130–142.
- 1050 Le Pichon, X. (1968). Seafloor spreading and continental drift. *J. Geophys. Res.*, 73(12):
 1051 3661-3697.
- 1052 Mandeville, C.W., Carey, S., Sigurdsson, H. (1996). Magma mixing, fractional crystallization
 1053 and volatile degassing during the eruption of Krakatau volcano, Indonesia. *J. Volcanol.*
 1054 *Geotherm. Res.* 74, 243-274.
- 1055 Metcalfe, I. (1990). Allochthonous terrane processes in Southeast Asia. *Phil. Trans. R. Soc.*
 1056 *Lond.* A331, 625-640.
- 1057 McCulloch, M.T., Gamble J.A. (1991). Geochemical and geodynamical constraints on
 1058 subduction zone magmatism. *Earth Planet. Sci. Lett.*, 102: 358-374.
- 1059 Miller, D.M., Goldstein, S.L., Langmuir, C.H. (1994). Cerium/lead and lead isotope ratios in
 1060 arc magmas and the enrichment of lead in the continents. *Nature* 368, 514-519.
- 1061 Moore, G.F., Curran, J.R., Moore, D.G., Karig, D.E. (1980). Variations in geologic structure
 1062 along the Sunda fore arc, northeastern Indian Ocean. In: Hayes, D.E. (ed) *The tectonic*
 1063 *and geological evolution of Southeast Asian seas and islands*. Am. Geophys. Union,
 1064 Washington, pp. 145-160.
- 1065 O’Nions, R.K., Frank, M., von Blanckenburg, F., Ling, H.-F. (1998). Secular variation of Nd
 1066 and Pb isotopes in ferromanganese crusts from the Atlantic, Indian and Pacific Oceans.
 1067 *Earth Planet. Sci. Lett.* 155, 15–28.
- 1068 Pacey, A., Macpherson, C.G., McCaffrey, K.J.W. (2013). Linear volcanic segments in the
 1069 central Sunda Arc, Indonesia, identified using Hough Transform analysis: Implications
 1070 for arc lithosphere control upon volcano distribution. *Earth and Planetary Science*
 1071 *Letters* 369-370, 24-33.
- 1072 Pearce, J.A., Peate, D.W. (1995). Tectonic implications of the composition of volcanic arc
 1073 magmas. *Annu. Rev. Earth Planet. Sci.*, 24: 251–285.

1074 Peccerillo, A., Dallai, L., Frezzotti, M.L., Kempton, P.D. (2004). Sr–Nd–Pb–O isotopic
1075 evidence for decreasing crustal contamination with ongoing magma evolution at Alicudi
1076 volcano (Aeolian arc, Italy): implications for style of magma-crust interaction and for
1077 mantle source compositions. *Lithos* 78, 217–233

1078 Plank, T., Langmuir, C.H. (1998). The chemical composition of subducting sediment and its
1079 consequences for the crust and mantle. *Chem. Geol.* 145, 325–394.

1080 Price, R.C., Kennedy, A.K., Riggs-Sneeringer, M., Frey, F.A. (1986). Geochemistry of
1081 basalts from the Indian Ocean triple junction: implications for the generation and
1082 evolution of Indian Ocean ridge basalts. *Earth Planet. Sci. Lett.*, 78: 379-396.

1083 Preece, K., Barclay, J., Gertisser, R., Herd, R.A. (2013). Textural and micro-petrological
1084 variations in the eruptive products of the 2006 dome-forming eruption of Merapi
1085 volcano, Indonesia: Implications for sub-surface processes. *J. Volc. Geotherm. Res.*
1086 261, 98–120.

1087 Ranero, C.R., Morgan, J.P., McIntosh, K., Reichert, C. (2003). Bending-related faulting and
1088 mantle serpentinization at the middle America trench. *Nature* 425, 367-373.

1089 Rehkämper, M., Hofmann, A.W. (1997). Recycled ocean crust and sediment in Indian Ocean
1090 MORB. *Earth Planet. Sci. Lett.*, 147: 93-106.

1091 Rittman, A. (1953). Magmatic character and tectonic position of the Indonesian volcanoes.
1092 *Bull. Volcanol.*, 14: 45-58.

1093 Rüpke, L.H., Phipps Morgan, J., Hort, M., Connolly, J.A.D. (2002). Are the regional
1094 variations in Central American arc lavas due to basaltic versus peridotitic slab sources
1095 of fluids? *Geology* 30, 1035-1038.

1096 Sakuyama, M. (1979). Evidence of magma mixing: petrological study of Shirouma-Oike calc-
1097 alkaline andesite volcano, Japan. *Journal of Volcanology and Geothermal Research* 5,
1098 179-208

1099 Singer, B.S., Leeman, W.P., Thirlwall, M.T., Rodgers, N.W. (1996), Does fracture zone
1100 subduction increase sediment flux and mantle melting in subduction zones? Trace
1101 element evidence from Aleutian arc basalt. *Subduction: Top to Bottom. Geophysical*
1102 *Monograph* 96, American Geophysical Union, 285-291.

1103 Sisson, T.W., Bronto S. (1998). Evidence for pressure-release melting beneath magmatic arcs
1104 from basalt at Galunggung, Indonesia. *Nature*, 391: 883-886.

1105 Sitorus, K. (1990). Volcanic stratigraphy and geochemistry of the Idjen Caldera Complex,
1106 East Java, Indonesia. MSc thesis, University of Wellington, New Zealand.

- 1107 Scholl, D.W., von Huene, R. (2009). Implications of estimated magmatic additions and
1108 recycling losses at the subduction zones of accretionary (non-collisional) and collisional
1109 (suturing) orogens. *Geological Society of London Special Publications* 318, 105–125.
- 1110 Smyth, H., Hall, R., Hamilton, J.P., and Kinny, P. (2005). East Java: Cenozoic basins,
1111 volcanoes and ancient basement: Jakarta, Proceedings, Indonesian Petroleum
1112 Association Annual Convention, 30th, p. 251–266.
- 1113 Smyth, H.R., Hamilton, P.J., Hall, R., and Kinny, P.D. (2007). The deep crust beneath island
1114 arcs: Inherited zircons reveal a Gondwana continental fragment beneath East Java,
1115 Indonesia: *Earth and Planetary Science Letters* 258, 269–282.
- 1116 Sun, S.-S. (1980). Lead isotopic study of young volcanic rocks from mid-ocean ridges, ocean
1117 islands and island arcs. *Royal Soc. Lon. Phil. Trans.*, 297, 409-445.
- 1118 Syracuse, E. M., Abers, G. A. (2006). Global compilation of variations in slab depth beneath
1119 arc volcanoes and implications, *Geochem. Geophys. Geosyst.*, 7, Q05017,
1120 doi:10.1029/2005GC001045.
- 1121 Tenthorey, E., Hermann, J. (2004). Composition of fluids during serpentinite breakdown in
1122 subduction zones: evidence for limited boron mobility (2004). *Geology* 32, 865-868.
- 1123 Thirlwall, M.F., Graham, A.M., Arculus, R.J., Harmon, R.S., Macpherson, C.G. (1996).
1124 Resolution of the effects of crustal assimilation, sediment subduction, and fluid
1125 transport in island arc magmas: Pb-Sr-Nd-O isotope geochemistry of Grenada, Lesser
1126 Antilles. *Geochim. Cosmochim. Acta*, 60(23), 4785-4810.
- 1127 Tregoning, P., Brunner, F.K., Bock, Y., Puntodewo, S.S.O., McCaffrey, R., Genrich, J.F.,
1128 Calais, E., Rais, J., Subarya, C. (1994). First geodetic measurement of convergence
1129 across the Java Trench. *Geophys. Res. Lett.* 21(19), 21352138.
- 1130 Troll, V.R., Deegan, F.M., Jolis, E.M., Harris, C., Chadwick, J.P., Gertisser, R., Schwarzkopf
1131 L.M., Borisova, A.Y., Bindeman, I.N., Sumarti, S., Preece, K. (2013). Magmatic
1132 differentiation processes at Merapi Volcano: inclusion petrology and oxygen isotopes, *J.*
1133 *Volcanol. Geotherm. Res.* 261, 38-49. doi: 10.1016/j.jvolgeores.2012.11.001.
- 1134 Turner, S., Foden, J. (2001). U, Th and Ra disequilibria, Sr, Nd and Pb isotope and trace
1135 element variations in Sunda arc lavas: predominance of a subducted sediment
1136 component. *Contrib. Mineral. Petrol.* 142, 43-57.
- 1137 van Bemmelen, R.W. (1949). The geology of Indonesia. Vol 1A. Government Printing
1138 Office, The Hague, 732 pp.

- 1139 van Gerven, M., Pichler, H. (1995). Some aspects of the volcanology and geochemistry of the
1140 Tengger Caldera, Java, Indonesia: eruption of a K-rich tholeiitic series. *Journal of*
1141 *Southeast Asian Earth Sciences* 11, 125-133.
- 1142 Vigouroux, N., Wallace, P.J., Williams-Jones, G., Kelley, K., Kent A.J.R., Williams-Jones,
1143 A.E. (2012). The sources of volatile and fluid-mobile elements in the Sunda arc: A melt
1144 inclusion study from Kawah Ijen and Tambora volcanoes, Indonesia, *Geochem.*
1145 *Geophys. Geosyst.* 13, Q09015, doi:10.1029/2012GC004192
- 1146 von Huene, R., Scholl, D.W. (1991). Observations at convergent margins concerning
1147 sediment subduction, subduction erosion, and the growth of continental crust. *Rev.*
1148 *Geophys.* 29, 279–316.
- 1149 Vroon, P.Z., Lowry, D., van Bergen, M.J., Boyce, A.J., Matthey, D.P. (2001). Oxygen isotope
1150 systematics of the Banda Arc: Low $\delta^{18}\text{O}$ despite involvement of subducted continental
1151 material in magma genesis. *Geochim. Cosmochim. Acta*, 65, 589-609.
- 1152 Vukadinovic, D., Sutawidjaja, I. (1995). Geology, mineralogy and magma evolution of
1153 Gunung Slamet Volcano, Java, Indonesia. *Journal of Southeast Asian Earth Sciences*,
1154 11, 135-164.
- 1155 Wakita, K. (2000). Cretaceous accretionary-collision complexes in central Indonesia: *Journal*
1156 *of Asian Earth Sciences* 18, 739–749.
- 1157 Wakita, K., Munasri, and Widoyoko, B. (1994). Cretaceous radiolarian from the Luk Ulo
1158 mélange complex in the Karangsambung area, Central Java, Indonesia: *Journal of*
1159 *Southeast Asian Earth Sciences* 9, 29–43.
- 1160 Wheller, G.E., Varne, R., Foden, J.D., Abbott, M.J. (1987). Geochemistry of Quaternary
1161 Volcanism in the Sunda-Banda arc, Indonesia, and three-component genesis of island-
1162 arc basaltic magmas. *J. Volc. Geotherm. Res.* 32, 137-160.
- 1163 White, W. M., Albarède, F., Télouk, P. (2000). High-precision analysis of Pb isotopic ratios
1164 using multi-collector ICPMS, *Chem. Geol.* 167, 257–270.
- 1165 Whitford, D. J. (1975). Strontium isotopic studies of the volcanic rocks of the Sunda arc,
1166 Indonesia, and their petrogenesis. *Geochim. Cosmochim. Acta* 39, 1287-1302.
- 1167 Whitford, D.J., Nicholls, I.A. (1976). Potassium variations in lavas across the Sunda arc in
1168 Java and Bali. In: R.W. Johnson (Editor), *Volcanism in Australasia*. Elsevier,
1169 Amsterdam, pp. 63-75.
- 1170 Whitford, D.J. (1982). Isotopic constraints on the role of subducted sialic material in
1171 Indonesian island-arc magmatism. *Geol. Soc. Am. Bull.* 93, 504-513.

1172 Woodhead, J.D., Hergt, J.M., Davidson, J.P., Eggins, S.M. (2001). Hafnium isotope evidence
1173 for ‘conservative’ element mobility during subduction processes. *Earth Planet. Sci. Lett.*
1174 192, 331–346.

1175

1176 **Figure Captions**

1177 Fig. 1. a) Tectonic setting of Java within the Sunda arc, Indonesia. Dashed lines with labels 1-
1178 4 represent the Mesozoic and Cenozoic growth of Sundaland suggested by Hall (2011): Line
1179 1: pre-Cretaceous Sundaland Core; Line 2: material added to the pre-Cretaceous Sundaland
1180 Core in the Early Cretaceous; Line 3: marks the eastern limit of material added in the Mid
1181 Cretaceous; Line 4: marks the eastern boundary of material added in the Early Miocene. The
1182 part of Line 2 crossing the Java Sea from Java to Borneo equates to Hamilton’s (1979) SE
1183 limit of Cretaceous continental crust. A-D (green fill) represent outcrops of Pre-Tertiary
1184 ophiolitic, accretionary-collision complexes in Java and SE Borneo (Hutchison, 1975;
1185 Wakita, 2000): A: Ciletuh; B: Luk Ulo (also known as Lok Ulo and Loh Ulo and
1186 Karangsambung); C: Jiwo Hills; D: Meratus and Pulau Laut. b) Bathymetric and
1187 topographic map of Java and the Java margin compiled from SRTM data. The visible
1188 displacement and retreat of the Java Trench by ~60 km to the north between 109°E and 115°E
1189 (area between dashed and solid black line (Kopp et al., 2006)) is attributed to the collision and
1190 subduction of oceanic basement relief of the Roo Rise (e.g., Kopp et al., 2006). Labels 1-5
1191 represent isolated bathymetric highs that are thought to represent seamounts already
1192 subducted at the Java Trench (Kopp et al., 2006). The inferred Progo-Muria lineament (Smyth
1193 et al., 2005; Smyth et al., 2007) and Central Java Fault (Chotin et al., 1984; Hoffmann-Rothe
1194 et al., 2001) are displayed and discussed in the text. The Eastern Wharton Basin and Argo
1195 Basin volcanic provinces (I-Seamount East field in Fig. 3; Hoernle et al., 2011) are delimited
1196 by white dashed lines. c) Topographic map of Java showing the location of major volcanoes.
1197 Volcanoes for which new Pb and O isotope data are presented in this study along with the
1198 location of the three local crustal sedimentary rocks (SED) are marked by red rectangles.
1199 Volcano names are consistent with those given by the Smithsonian Institution, Global
1200 Volcanism Program (<http://www.volcano.si.edu/>). Division of volcanoes in to West, Central
1201 and East as defined in the text.

1202

1203 Fig. 2. Along-arc variations for selected Javanese volcanoes showing: a) Subducting seafloor
1204 age, b) Average slab dip, c) Slab depth and, d) Distance from trench using data from Syracuse
1205 and Abers (2006). Dashed vertical lines denote West, Central and East Java boundaries used

1206 in the manuscript and detailed in Section 3. Arrow shows volcanoes located within the plate
1207 margin region affected by the collision and subduction of the Roo Rise (Fig. 1b), an area of
1208 oceanic basement relief, as delimited by Kopp et al. (2006). Volcanoes for which geochemical
1209 data are used within this study are shown by bold outline symbols and defined in the key.

1210

1211 Fig. 3. a) and b) Pb isotope compositions of Salak, Gede, Galunggung, Merbabu, Merapi and
1212 Ijen (this study, colour-filled symbols) compared to published Javanese volcanic rocks
1213 (Edwards 1990, 1993; Woodhead et al., 2001), Indian Ocean mid ocean ridge basalt (I-
1214 MORB: Rehkämper and Hofmann, 1997; Ito et al., 1987; Price et al., 1986; Chauvel and
1215 Blichert-Toft, 2001), Indian Ocean sediments (I-SED: Ben Othman et al., 1989; Gasparon and
1216 Varne, 1998), Indian Ocean ferromanganese nodule crusts (I-Mn crusts: Frank and O’Nions,
1217 1998; O’Nions et al., 1998) and Indian Ocean Seamounts (I-Seamount: Outsider Seamount
1218 and Cocos-Keeling, Vening-Meinesz, Eastern Wharton Basin and Argo Basin Volcanic
1219 Provinces: Hoernle et al., 2011). The composition of seamounts subducting at the Java Trench
1220 is represented by the Eastern Wharton Basin and Argo Basin Volcanic Provinces (I-Seamount
1221 East). Also plotted are the estimated altered oceanic crust composition (AOC) from Edwards
1222 et al. (1993), estimated bulk Java subducted sediment (Plank and Langmuir, 1998), global
1223 subducted sediment (GLOSS; Plank and Langmuir, 1998). Local crustal rocks from West
1224 Java (marl, volcanoclastic sandstone and mudstone) (this study) along with calcareous
1225 sediments from Central Java (Gertisser and Keller, 2003a) are shown. The calc-silicate
1226 xenolith is from a Merapi volcanic rock (Gertisser and Keller, 2003a). Sumatran intrusive
1227 rocks are from Gasparon and Varne (1995). An example bulk mixing line (0-100%) is shown
1228 between average I-MORB source (Pb: 0.07 ppm, $^{206}\text{Pb}/^{204}\text{Pb}$: 17.899, $^{207}\text{Pb}/^{204}\text{Pb}$: 15.471,
1229 $^{208}\text{Pb}/^{204}\text{Pb}$: 37.763, n = 43) and bulk Java subducting sediment (Pb: 25.5 ppm, $^{206}\text{Pb}/^{204}\text{Pb}$:
1230 18.990, $^{207}\text{Pb}/^{204}\text{Pb}$: 15.741, $^{208}\text{Pb}/^{204}\text{Pb}$: 39.328, Plank and Langmuir, 1998). c) and d) show
1231 the new Pb isotope data for Salak, Gede, Galunggung, Merbabu, Merapi and Ijen volcanic
1232 rocks (large symbols) and new local crust data from West Java (marl, volcanoclastic sandstone
1233 and mudstone) with other published Javanese (including Krakatau) volcano Pb isotope data
1234 (small symbols; Edwards, 1990, 1993; Woodhead et al., 2001).

1235

1236 Fig. 4. a) Olivine (ol), clinopyroxene (cpx) and plagioclase (plag) mineral separate $\delta^{18}\text{O}$ and
1237 whole-rock (WR) (inset) $\delta^{18}\text{O}$ values versus $^{206}\text{Pb}/^{204}\text{Pb}$ for Javanese volcanic rocks. Whole-
1238 rock Merapi Pb isotope data is from this study and the O isotope data is from Gertisser and

1239 Keller (2003a). Mineral data are plotted as measured $\delta^{18}\text{O}$ values, rather than calculated
1240 equilibrium melt values, due to the potential uncertainty in mineral-melt fractionation factors
1241 compared to mineral-mineral fractionation factors (Eiler, 2001). b) Along-arc variations in
1242 $\delta^{18}\text{O}$ of Javanese volcano mineral separates and whole-rock samples (inset). The Merbabu
1243 volcanic rocks are amongst the highest $\delta^{18}\text{O}$ whole-rock values yet reported in Java. S: Salak
1244 (Handley et al., 2008a), Ge: Gede (Handley et al., 2010), Gu: Guntur (Edwards, 1990;
1245 Macpherson et al., submitted), Ga: Galunggung (Gerbe et al., 1992), C: Cereme (Edwards,
1246 1990), M: Merapi (Gertisser and Keller, 2003a; Troll et al., 2013), K: Kelut (Jeffery et al.,
1247 2013), I: Ijen (Handley et al., 2007). The upper mantle range of $+5.5 \pm 0.2\text{‰}$ for
1248 clinopyroxene is taken from Eiler (2001). c) Javanese clinopyroxene mineral separate $\delta^{18}\text{O}$
1249 values versus whole-rock $^{206}\text{Pb}/^{204}\text{Pb}$. Simple bulk-mixing curves are shown for mixing
1250 between depleted mantle source and local Indian Ocean sediment (model A) and Javanese arc
1251 magma with local arc crust (model B). Tick marks indicate the percentage of crustal material
1252 added to the depleted mantle source and arc magma. Data used in mixing calculations:
1253 Depleted mantle source: Pb = 0.07 ppm; $^{206}\text{Pb}/^{204}\text{Pb} = 17.899$ (average I-MORB composition
1254 used in Fig. 3); O = 43.8 wt% (Vroon et al., 2001); $\delta^{18}\text{O} = +5.5\text{‰}$ (Eiler, 2001). Local
1255 subducted sediment: Pb = 25.5 ppm; $^{206}\text{Pb}/^{204}\text{Pb} = 18.990$ (Plank and Langmuir, 1998); O =
1256 50.2 wt% (Vroon et al., 2001); $\delta^{18}\text{O} = 18.7\text{‰}$ (Vroon et al., 2001; based on DSDP site 262
1257 data). Arc magma: Pb = 6.1 ppm (KI 69, Handley et al., 2007); $^{206}\text{Pb}/^{204}\text{Pb} = (\text{KI 69, Table 1})$;
1258 O = 50.2 wt% (Vroon et al., 2001); $\delta^{18}\text{O} = +5.5\text{‰}$. Local arc crust: Pb = 4.95 ppm (SEDA,
1259 Table 3); $^{206}\text{Pb}/^{204}\text{Pb} = 18.722$ (SEDA, Table 1); O = 50.2 wt% (Vroon et al., 2001); $\delta^{18}\text{O} =$
1260 19‰ (representative of local calcareous sedimentary arc crust given by Gertisser and Keller,
1261 2003a). Inset diagram shows the expected mixing trends for crustal assimilation (dashed
1262 lines) versus subducted sediment input (solid lines) for crustal materials with variable
1263 $^{206}\text{Pb}/^{204}\text{Pb}$ ratios. DM = depleted mantle source.

1264

1265 Fig. 5. Variation of whole-rock Pb isotope ratios with SiO_2 content for Salak, Gede,
1266 Galunggung, Merapi, Merbabu and Ijen volcanic rocks relative to other Javanese volcanic
1267 rocks (Edwards 1990, 1993; Woodhead et al., 2001). SiO_2 data, for the samples with new Pb
1268 isotope data, are from Sitorus (1990), Turner and Foden (2001), Gertisser and Keller (2003a),
1269 Handley et al. (2007; 2008a; 2010; 2011), Preece et al. (2013) plus ME07-53: 55.40 wt%,
1270 M11-05: 54.08 wt%, M11-18: 55.72 wt%. The central Java upper crustal calcareous
1271 sedimentary rocks of Gertisser and Keller (2003a) are plotted on the Y-axis (SiO_2 contents not

1272 available). Arrows labelled SH, AFC and FC indicate the hypothesised data trends related to:
1273 heterogeneity in the mantle source (SH), combined assimilation and fractional crystallisation
1274 (AFC) and fractional crystallisation (FC). AFC trends can be positive or negative depending
1275 on the Pb isotope ratio of the assimilated material. AFC 1: high Pb isotope ratio assimilant
1276 e.g., continental crust; AFC 2: assimilation of local West and Central Javanese carbonaceous
1277 sedimentary rocks; AFC 3: assimilation of more isotopically primitive arc rocks or ophiolitic-
1278 type arc crust.

1279

1280 Fig. 6. $\text{Na}_2\text{O}+\text{K}_2\text{O}$ versus SiO_2 for Javanese volcanic rocks and local, West Java upper crustal
1281 rocks (marl, volcanoclastic sandstone and mudstone). Large symbols show the volcanoes with
1282 new Pb isotope data presented in this study. Arrows (upper left) show the expected
1283 differentiation path for fractional crystallisation of clinopyroxene (FC Cpx) and olivine (FC
1284 Ol) and indicate the desilication effect of carbonate assimilation in a closed system depending
1285 on the availability (Carb Assim (Ol/MgO)) or not (Carb Assim (no Ol)) of MgO in the magma,
1286 following Iacono Marziano et al. (2008). Java data sources as in Figs. 3 and 5 plus Claproth
1287 (1989), Camus et al. (1987), Gerbe et al. (1992), Vukadinovic and Sutawidjaja (1995),
1288 Hartono (1996), van Gerven and Pichler (1995), Mandeville et al. (1996), Carn and Pyle
1289 (2001), Jeffery et al. (2013) and Abdurrachman and Yamamoto (2012).

1290

1291 Fig. 7. Along-arc a) Pb isotope, b) Sr isotope and, c) Ba/Hf and Ba/Nb (inset) variations in
1292 Javanese volcanic rocks. Note the similarity between the along-arc O isotope (Fig. 4b,
1293 clinopyroxene or plagioclase mineral data) and Sr isotope patterns compared to the along-arc
1294 Pb isotope pattern. Data sources given in Figs. 3, 5, 6 plus additional data from Whiford
1295 (1975) and Abdurrachman and Yamamoto (2012). Da: Danau Complex; TP:
1296 Tangkubanparahu; P: Papandayan; Gu: Guntur; Ci: Cikuray; Ga: Galunggung; C: Cereme; Sl:
1297 Slamet; D: Dieng Volcanic Complex; Sun: Sundoro; Su: Sumbing; Un: Ungaran; Law: Lawu;
1298 Ke: Kelut; Se: Semeru; Lam: Lamongan. Hf concentration data is not available for Tengger
1299 Caldera but this volcano is plotted in the East Java field (112.95°E) in the insert Ba/Nb
1300 diagram (van Gerven and Pichler, 1995).

1301

1302 Fig. 8. a) Ba concentration versus SiO_2 content in Javanese volcanic rocks. Large symbols
1303 show the volcanoes with new Pb isotope data presented in this study. Data sources are given
1304 in Figs. 3 and 7. b) Pb isotope ratio versus Ba/Hf versus in Javanese volcanic rocks. Data
1305 sources are given in Figs. 3 and 7. Symbols as those given in Fig. 3. Local Indian Ocean

1306 sediment (I-SED) end members used in bulk-mixing models: A: Lower Cretaceous claystone
1307 (29-2:29-31), Pb: 15 ppm, $^{206}\text{Pb}/^{204}\text{Pb}$: 18.576, Ba: 1063 ppm, Hf: 2.69 ppm (Gasparon and
1308 Varne, 1998); B: Quaternary terrigenous mud (VM33-79) Pb: 17 ppm, $^{206}\text{Pb}/^{204}\text{Pb}$: 18.67, Ba:
1309 129 ppm, Hf: 3.04 ppm (Gasparon and Varne, 1998); C: Bulk Java Sediment, Pb: 25.5 ppm,
1310 $^{206}\text{Pb}/^{204}\text{Pb}$: 18.99, Ba: 1068 ppm, Hf: 4.73 ppm (Plank and Langmuir, 1998). Depleted I-
1311 MORB mantle source: Pb: 0.07 ppm, $^{206}\text{Pb}/^{204}\text{Pb}$: 17.899, Ba: 2.74 ppm, Hf: 0.25 ppm
1312 (Rehkämper and Hofmann, 1997; Ito et al., 1987; Price et al., 1986; Chauvel and Blichert-
1313 Toft, 2001). Tick marks show the percentage of bulk sediment added (increments are 0.5%,
1314 1%, 1.5%, 2%, 2.5%, 3%, 5%, 10%, 50%, 100%) to the depleted I-MORB source. Box with
1315 arrows (lower right) exemplifies the anticipated maximum overprint on Ba/Hf and $^{206}\text{Pb}/^{204}\text{Pb}$
1316 from crustal assimilation at Gede Volcanic Complex, West Java.

1317

1318 Fig. 9. Ba/Hf versus La/Yb in Javanese volcanic rocks. Data sources are given in Fig. 7.

Table 1. Pb isotope data of Javanese volcanic and sedimentary rocks

Province	Volcano	Eruptive Vent/Age	Sample	$^{206}\text{Pb}/^{204}\text{Pb}$	$^{207}\text{Pb}/^{204}\text{Pb}$	$^{208}\text{Pb}/^{204}\text{Pb}$
West Java	Salak	Central Vent	S109	18.827	15.703	39.222
West Java	Salak	Central Vent	S110A	18.799	15.676	39.150
West Java	Salak	Central Vent	S111	18.814	15.700	39.199
West Java	Salak	Side Vent	S103	18.703	15.670	39.018
West Java	Salak	Side Vent	S107B	18.832	15.704	39.222
West Java	Salak	Pre-Salak	S100	18.816	15.697	39.187
West Java	Gede Volcanic Complex	Young Gede (KR)	G23	18.879	15.715	39.281
West Java	Gede Volcanic Complex	Young Gede (KR)	G25	18.830	15.688	39.155
West Java	Gede Volcanic Complex	Young Gede (KR)	G40	18.870	15.710	39.262
West Java	Gede Volcanic Complex	Young Gede (OV)	G20	18.867	15.707	39.270
West Java	Gede Volcanic Complex	Young Gede (OV)	G36A	18.863	15.706	39.236
West Java	Gede Volcanic Complex	Old Gede	G17	18.837	15.699	39.194
West Java	Gede Volcanic Complex	Old Gede	G46	18.873	15.708	39.262
West Java	Gede Volcanic Complex	Pangrango	G35	18.938	15.733	39.400
West Java	Gede Volcanic Complex	Gegerbentang	G33	18.914	15.725	39.352
West Java	Gede Volcanic Complex	Older Quaternary	G52	18.774	15.687	39.117
West Java	Sedimentary Rock	Marl	SEDA	18.722	15.665	38.944
West Java	Sedimentary Rock	Volcanic Sandstone	SEDB	18.687	15.663	38.968
West Java	Sedimentary Rock	Mudstone	SEDC	18.785	15.675	38.971
West Java	Galunggung*	AD 1982 eruption	VB82	18.7991	15.6987	39.1939
West Java	Galunggung*	AD 1918 eruption	4AK	18.7524	15.6807	39.1007
Central Java	Merapi	AD 2006 eruption	ME07-53	18.762	15.693	39.147
Central Java	Merapi	AD 2006 eruption	ME08-07	18.766	15.697	39.157
Central Java	Merapi	AD 2006 eruption	ME08-14	18.762	15.692	39.143
Central Java	Merapi	AD 2010 eruption	M11-05	18.770	15.696	39.162
Central Java	Merapi	AD 2010 eruption	M11-12	18.762	15.694	39.147
Central Java	Merapi	AD 2010 eruption	M11-18	18.762	15.692	39.125
Central Java	Merapi	AD 2010 eruption	M11-27-5	18.760	15.692	39.137
Central Java	Merapi	AD 2010 eruption	M11-28b	18.765	15.697	39.153
Central Java	Merapi*	High-K, Recent-Historical	M97-068	18.763	15.694	39.141
Central Java	Merapi*	High-K, Holocene	M98-096	18.771	15.697	39.156
Central Java	Merapi*	Med-K, Holocene	M96-137	18.759	15.695	39.139
Central Java	Merapi*	Med-K, Holocene	M96-073	18.755	15.692	39.134
Central Java	Merapi*	Med-K, Merapi-Somma	M95-026	18.769	15.693	39.130
Central Java	Merbabu	S-sector (Patran)	MB-1	18.828	15.710	39.245
Central Java	Merbabu	S-sector (Jrahah-Selo)	MB-2	18.802	15.690	39.173
Central Java	Merbabu	SW-sector (SE of Candimulyo)	MB-6	18.805	15.691	39.182
Central Java	Merbabu	N-sector (E of Kopeng)	MB-16	18.756	15.665	39.040
Central Java	Merbabu	N-sector (NE of Getasan)	MB-22	18.755	15.669	39.045
Central Java	Merbabu	E-sector (N or Penggung)	MB-28	18.807	15.696	39.188
East Java	Ijen Volcanic Complex	Djampit (Caldera Rim)	KI 69	18.526	15.617	38.768
East Java	Ijen Volcanic Complex	Djampit (Caldera Rim)	KI 137	18.551	15.611	38.753
East Java	Ijen Volcanic Complex	Djampit (Caldera Rim)	KI 136	18.540	15.611	38.747
East Java	Ijen Volcanic Complex	Merapi (Caldera Rim)	KI 116	18.578	15.626	38.802
East Java	Ijen Volcanic Complex	Merapi (Caldera Rim)	KI 194	18.598	15.628	38.836
East Java	Ijen Volcanic Complex	Kawah Ijen	KI 190	18.602	15.635	38.861
East Java	Ijen Volcanic Complex	Glaman (Intra Caldera)	KI 35	18.574	15.624	38.806
East Java	Ijen Volcanic Complex	Anyar (Intra Caldera)	KI 142	18.563	15.623	38.789

Further sample information is available in Handley et al. (2007) for Ijen, Handley et al. (2008) for Salak, Gertisser et al. (2003a, 2003b) and Preece et al. (2013) for Merapi, Handley et al. (2011) for Merbabu and Handley et al. (2010) for Gede Volcanic Complex.

KR: Kawa Ratu; OV: Other Vents Group

*samples re-analysed in this study for which previously published TIMS Pb isotope data is available in Gertisser et al. (2003a) for Merapi and Turner et al. (2001) for Galunggung.

Data comparison between the new and previously published Pb isotope data is provided in the Appendix.

Table 2. Whole-rock oxygen isotope compositions of Merbabu volcanic rocks

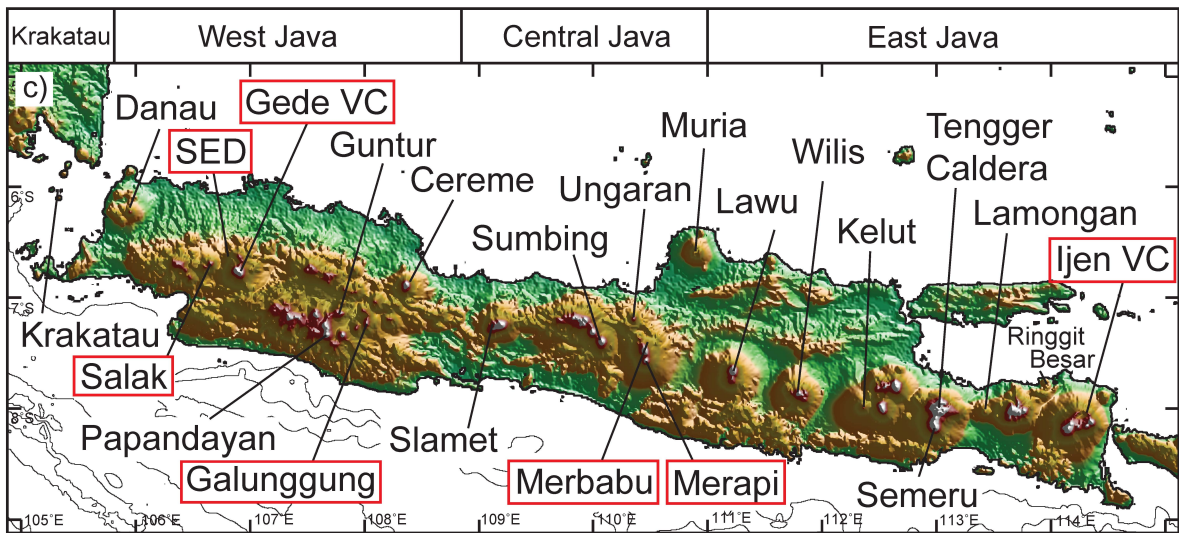
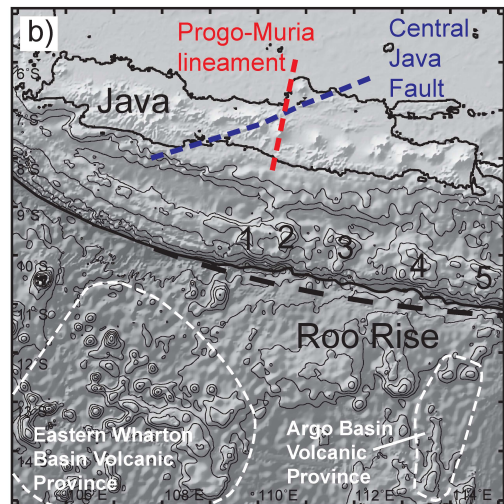
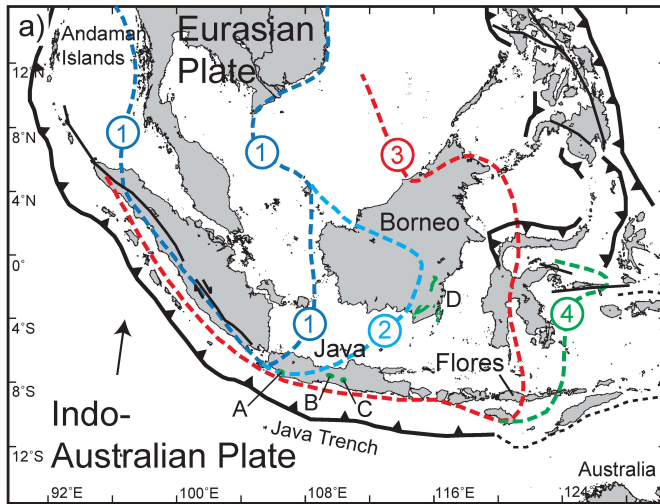
Sample	$\delta^{18}\text{O}$
MB-1	+7.3
MB-2	+6.4
MB-6	+7.2
MB-16	+8.4
MB-22	+8.1
MB-28	+6.8

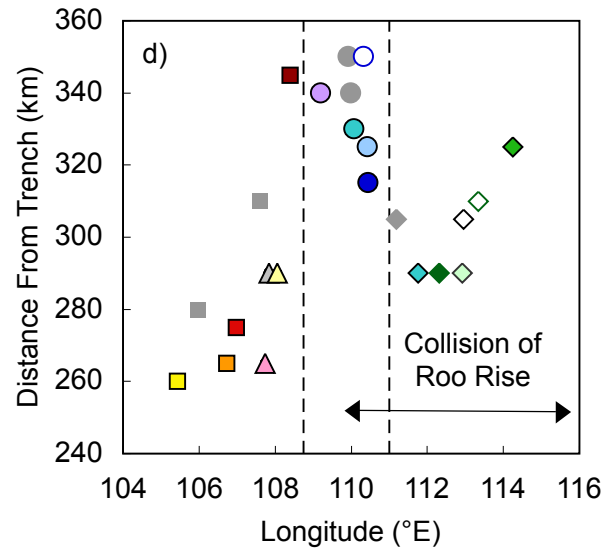
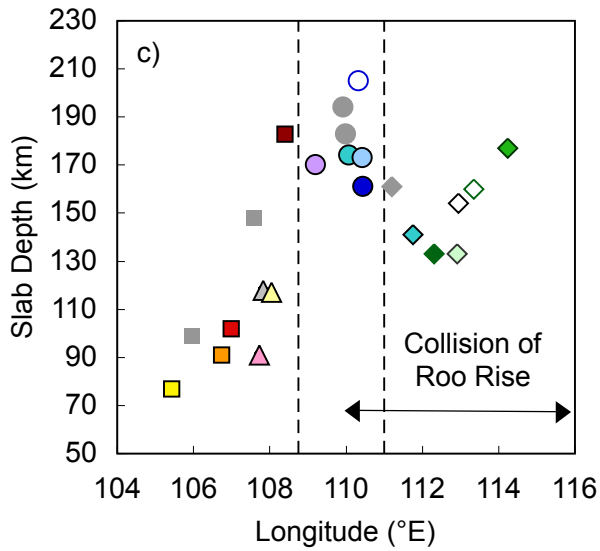
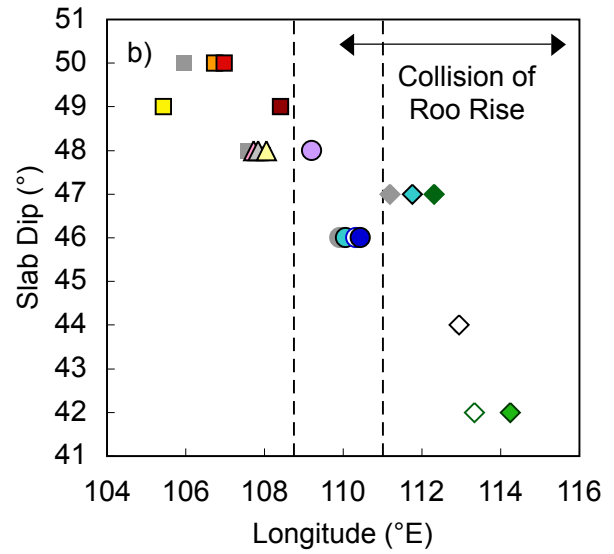
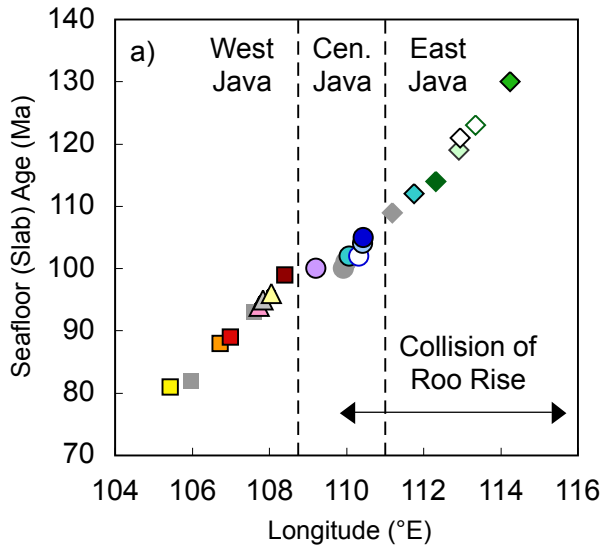
O isotope data reported as per mil (‰)

Table 3. Major element, trace element and Sr-Nd-Hf isotope data of West Java upper crust sedimentary rocks

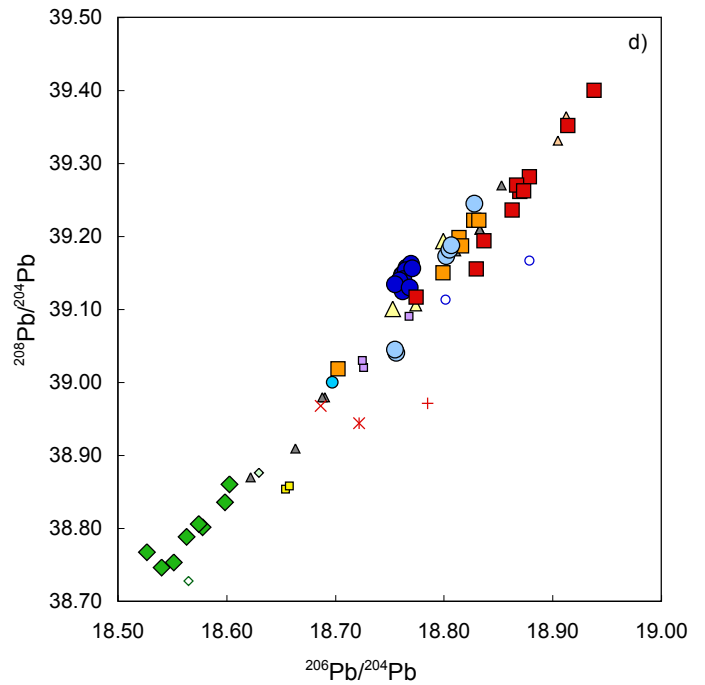
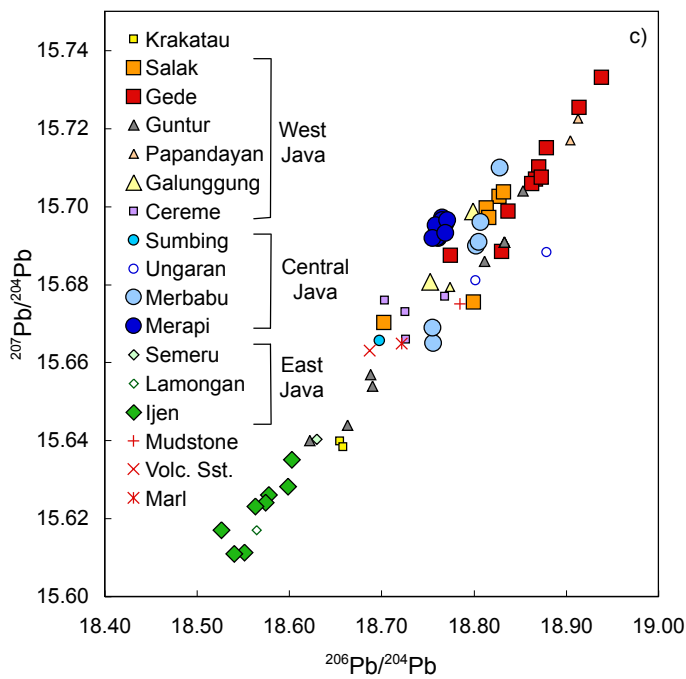
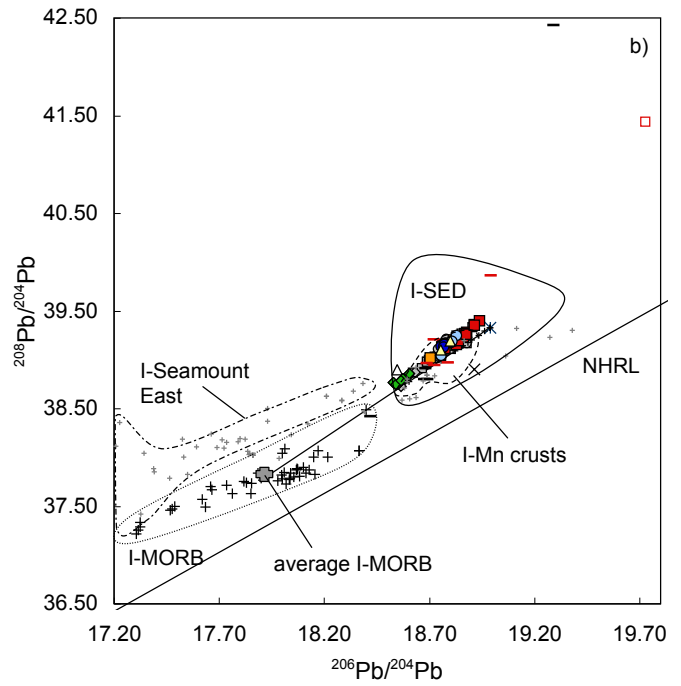
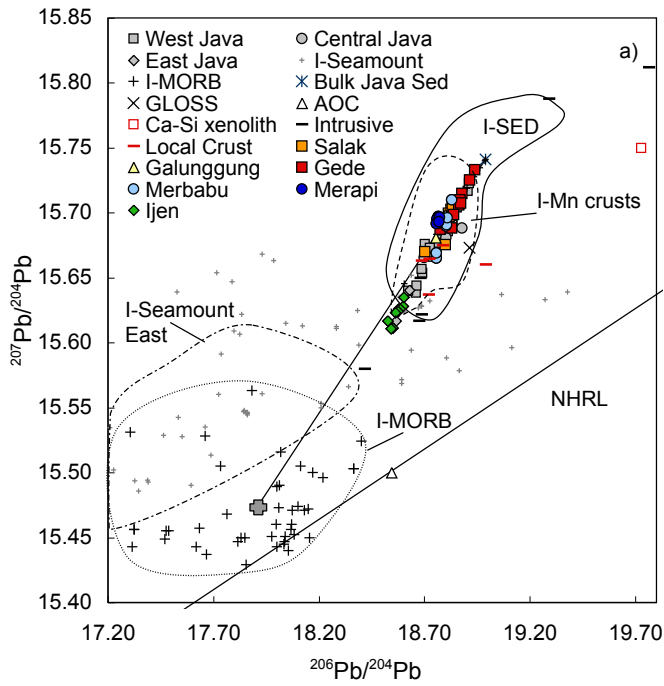
Sample	SED-A	SED-B	SED-C
Latitude	06°37'30.7"S	06°37'30.7"S	06°37'30.7"S
Longitude	106°53'06.4"E	106°53'06.4"E	106°53'06.4"E
Elevation	438 ± 7m	438 ± 7m	438 ± 7m
Rock Type	Marl	Volcaniclastic sandstone	Mudstone
SiO ₂	14.99	51.42	55.74
Al ₂ O ₃	5.61	20.67	22.29
Fe ₂ O ₃	4.94	6.61	6.53
MgO	8.63	2.10	2.13
CaO	28.71	6.73	0.72
Na ₂ O	0.55	2.93	0.36
K ₂ O	0.34	0.65	2.01
TiO ₂	0.21	0.78	0.87
MnO	1.64	0.11	0.05
P ₂ O ₅	0.14	0.17	0.05
LOI	32.97	6.47	9.0
Total	98.72	98.64	99.75
Na ₂ O+K ₂ O	0.886	3.576	2.367
Sc	2.5	12.8	17.0
V	33	34	118
Cr	7.7	3.0	47.8
Co	3.5	8.0	14.1
Ni	7.5	4.6	23.5
Cu	5.6	11.3	14.6
Zn	27.6	76.6	88.4
Rb	9.0	10.0	76.4
Sr	373	372	74
Y	29.6	24.1	20.1
Zr	66	186	165
Nb	3.4	15.4	10.2
Cs	0.5	0.2	6.8
Ba	73.8	141.6	155.7
La	15.8	27.3	27.7
Ce	30.3	61.2	62.3
Pr	3.84	8.05	7.15
Nd	16.2	32.3	27.7
Sm	3.45	6.20	5.35
Eu	0.83	2.06	1.14
Gd	3.66	4.98	4.42
Tb	0.60	0.81	0.69
Dy	3.80	4.69	3.93
Ho	0.85	0.95	0.80
Er	2.55	2.57	2.26
Tm	0.43	0.41	0.37
Yb	2.87	2.70	2.41
Lu	0.51	0.45	0.40
Hf	1.46	5.05	4.01
Ta	0.26	0.99	0.83
Pb (total)	4.95	13.6	23.9
Th	2.93	7.31	12.4
U	1.91	1.73	2.21
Ba/Hf	50.7	28.1	38.8
⁸⁷ Sr/ ⁸⁶ Sr	0.704339	0.704979	0.709587
2SE	0.000008	0.000011	0.000011
¹⁴³ Nd/ ¹⁴⁴ Nd	0.512806	0.512792	0.512552
2SE	0.000032	0.000007	0.000006
¹⁷⁶ Hf/ ¹⁷⁷ Hf	0.283313	0.283077	0.282966
2SE	0.000082	0.000007	0.000007

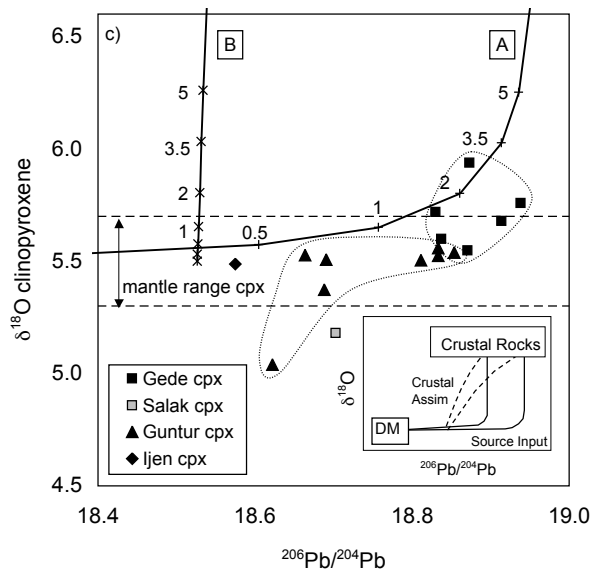
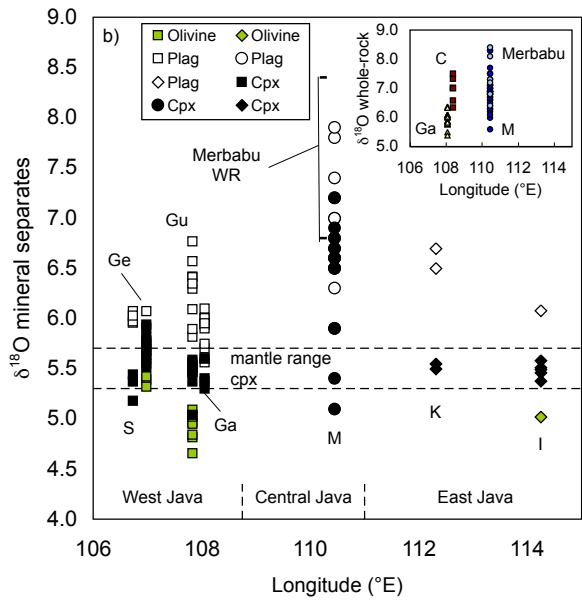
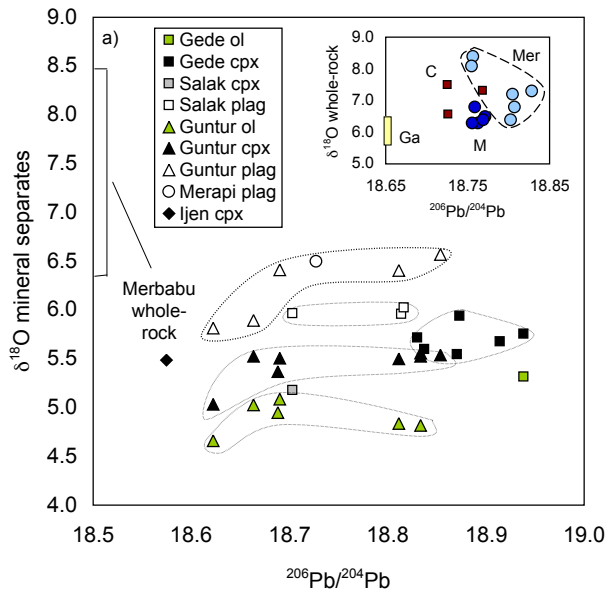
Major element contents are given in wt% and trace element concentrations are given in ppm.

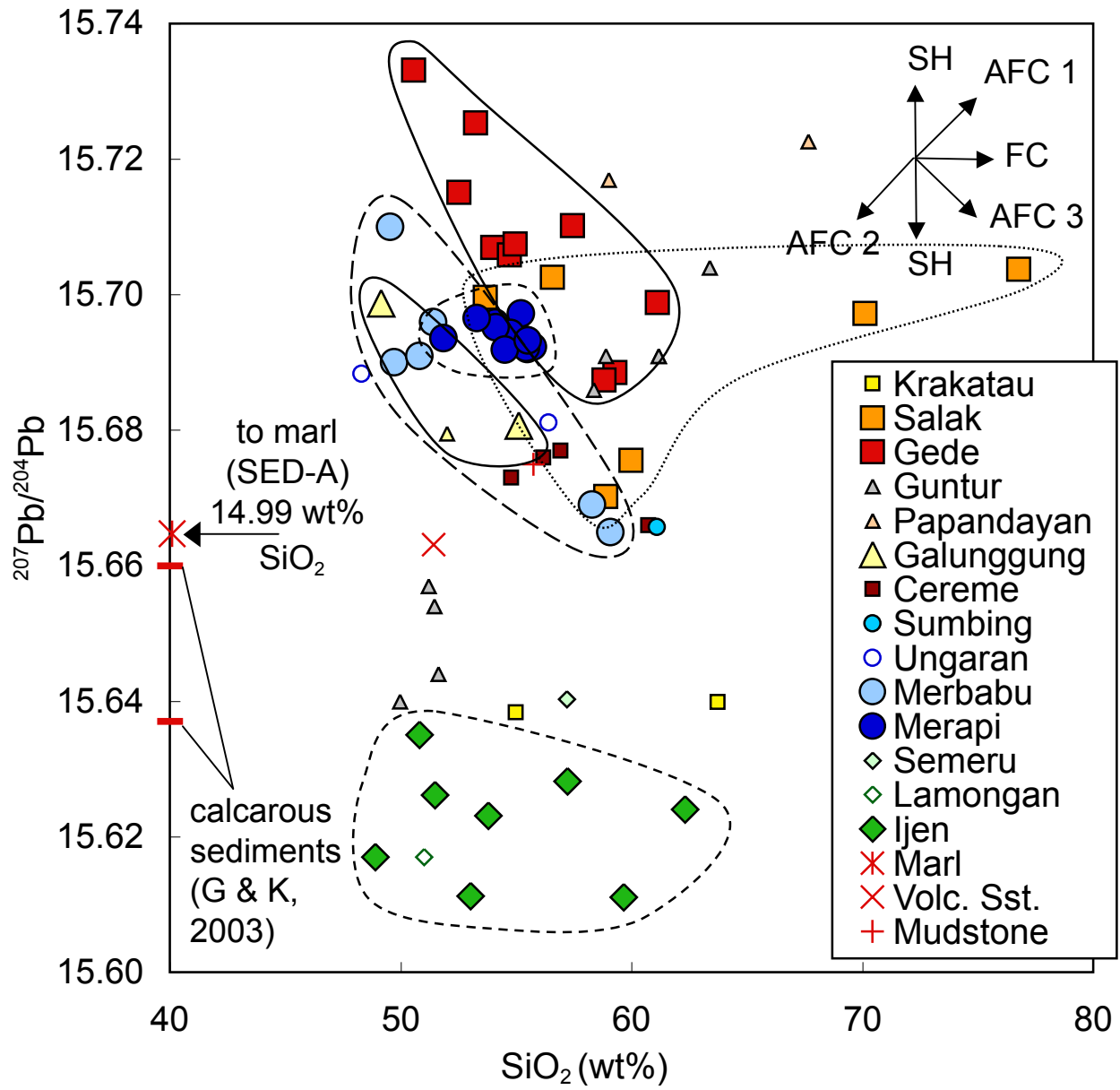


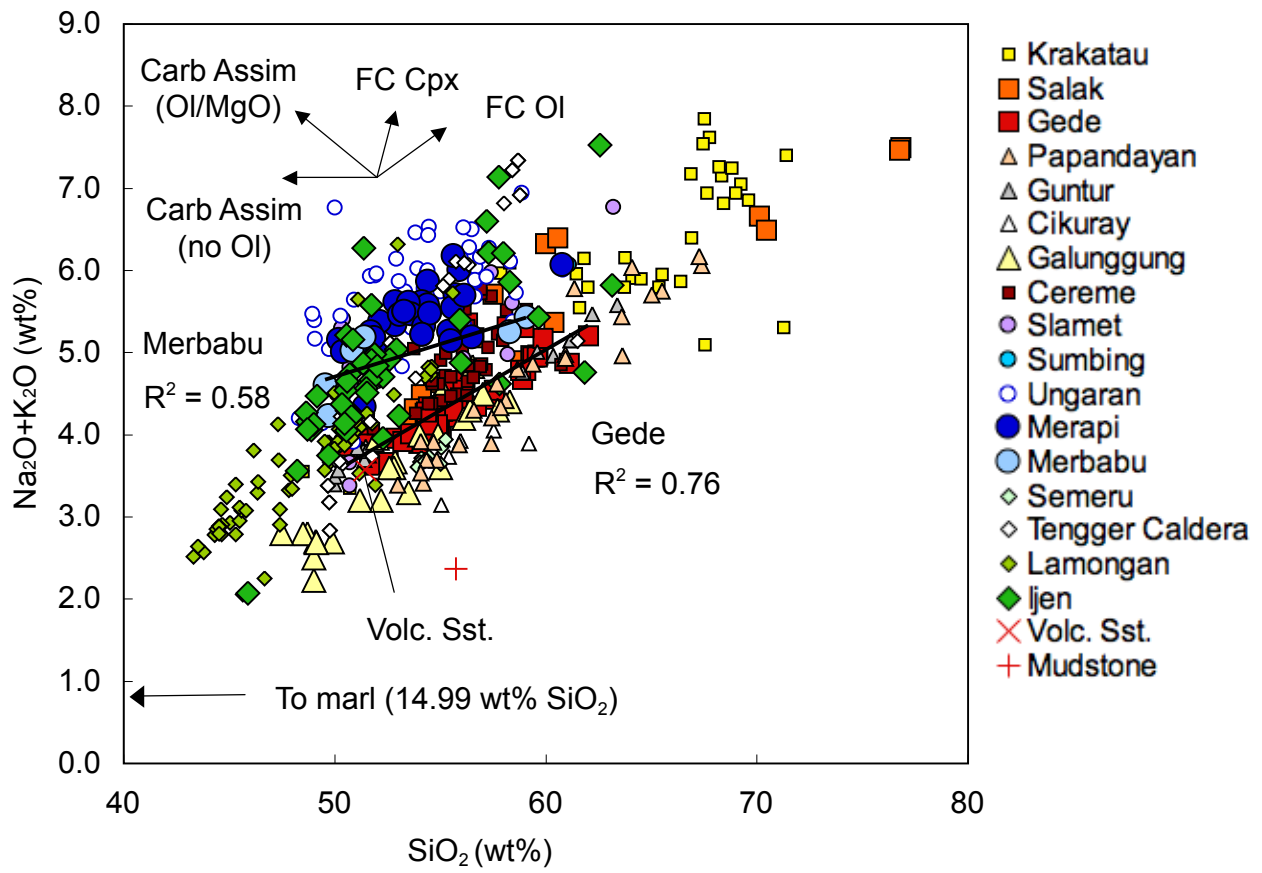


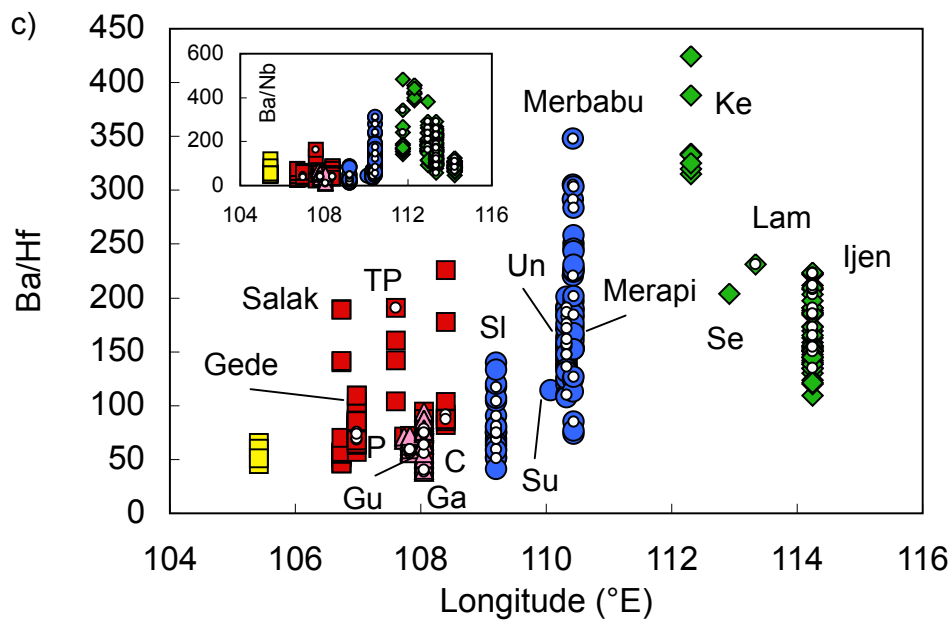
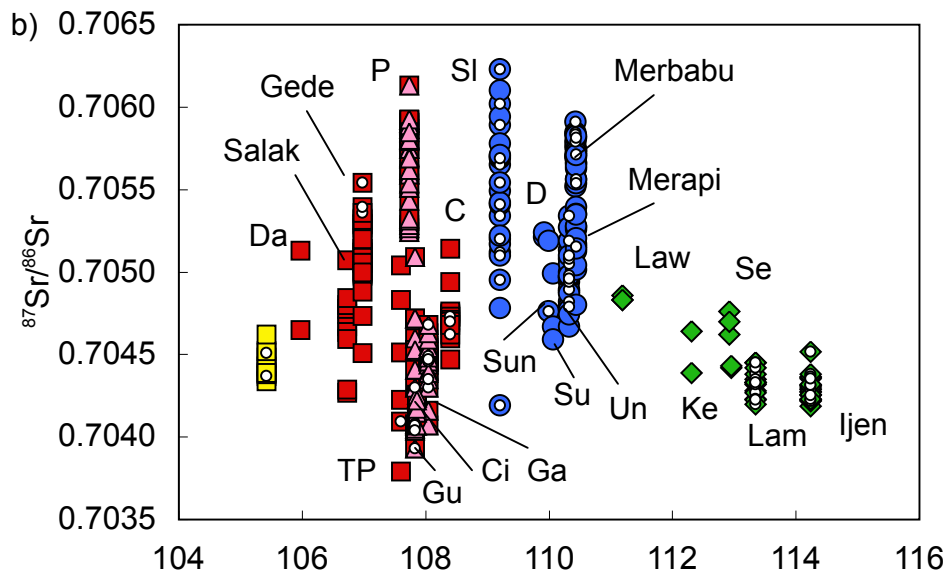
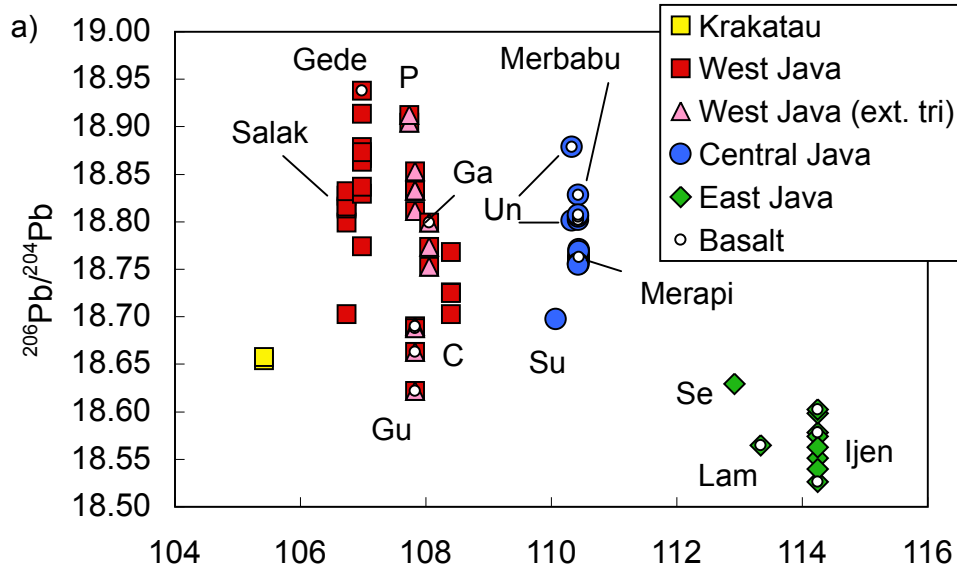
- | | |
|--------------|-------------------|
| ■ Krakatau | ■ Salak |
| ■ Gede | △ Guntur |
| △ Papandayan | △ Cikuray |
| △ Galunggung | ■ Cereme |
| ○ Slamet | ● Sumbing |
| ○ Ungaran | ● Merapi |
| ○ Merbabu | ◇ Wilis |
| ◇ Semeru | ◇ Lamongan |
| ◇ Ijen | ◇ Tengger Caldera |
| ◇ Kelut | |

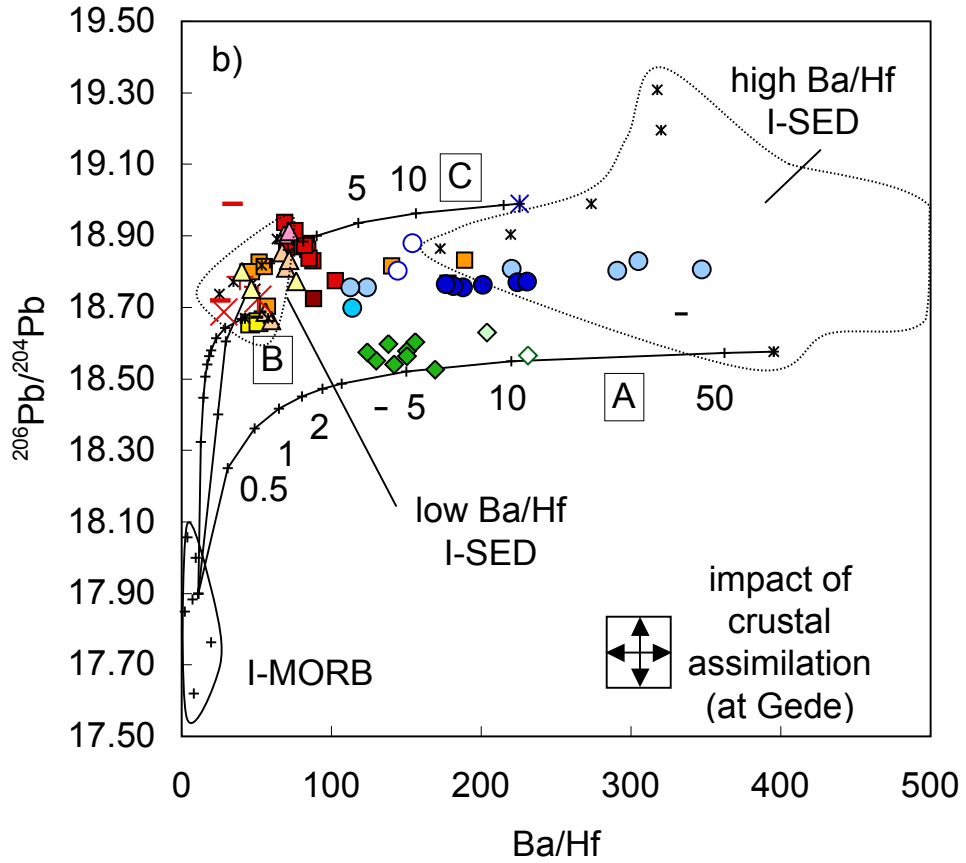
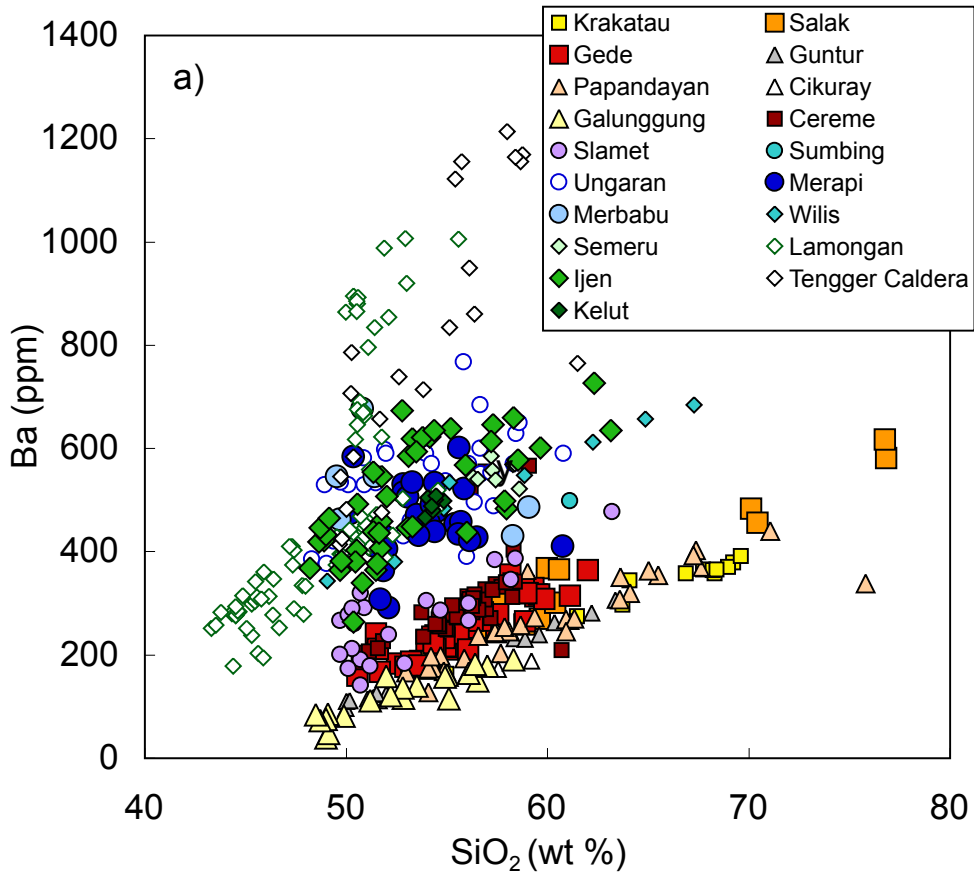


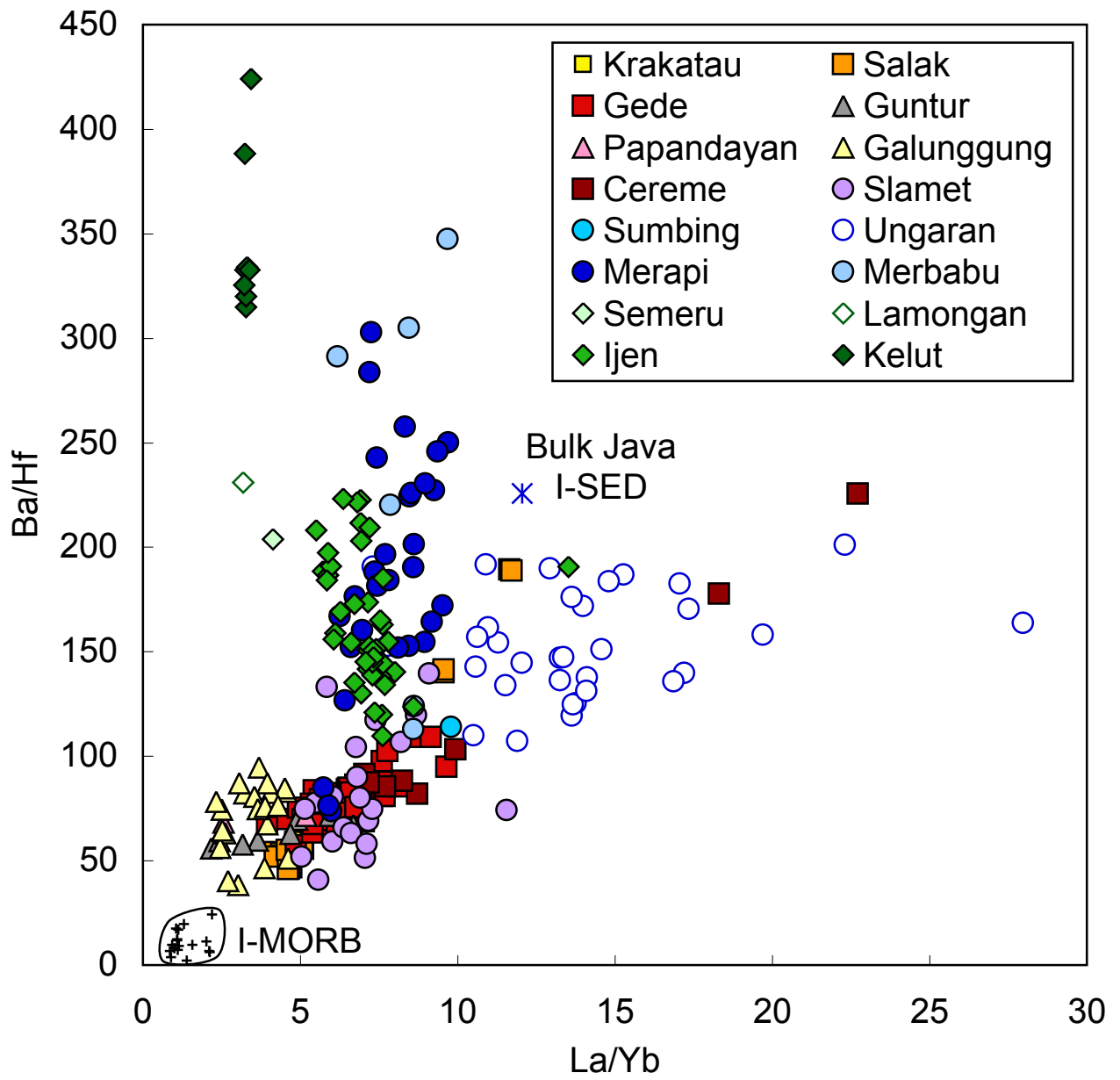












Appendix

Comparison of re-analysed Pb isotope ratios with previously published data

An inter-laboratory comparison of Pb isotope data by Thirlwall (2000) revealed significant variation in reported Pb isotope ratios for the same samples (up to 30 times the supposed reproducibility based upon replicate analyses of NIST SRM 981). These large differences were attributed to inadequate fractionation corrections and/or environmental contamination of rock powder. Woodhead and Hergt (2000) also showed that the conventional corrections for (unspiked) thermal ionisation mass spectrometer (TIMS) induced Pb-isotopic fractionation often result in a loss of accuracy due to the different fractionation behaviours of pure Pb reference materials (NIST SRM 981, 982) and natural rock samples. Therefore, rock powders from Galunggung and Merapi volcanoes with previously published Pb isotope data were re-analysed in this study to facilitate comparison between data sets collected in different laboratories using different methods and instrumentation (e.g., Tl-doped multi-collector inductively-coupled plasma mass spectrometry (MC-ICP-MS) with sample-standard bracketing data versus unspiked, conventionally fractionation-corrected TIMS data).

Table A1 compares the analytical techniques employed for the previously published (TIMS) and new (re-analysed) Pb isotope data for Galunggung and Merapi. The new and previously published Pb isotope data are presented in Table A2 and Figure A1.

Table A1. Summary of analytical methods for new (re-analysed) and previously published data for Galunggung and Merapi volcanoes

Volcano	Data Source	Instrument and Laboratory	Pre-sample Treatment	Fractionation Correction Control
Galunggung	Turner and Foden (2001)	TIMS (Open University)	None	~1‰ per atomic mass unit using NIST SRM 981 values from Todt et al. (1993)
Merapi	Gertisser and Keller (2003a)	TIMS (Universität Tübingen)	None	1‰ per atomic mass unit using NIST SRM 981 (value not given)
Galunggung and Merapi	This study	MC-ICP-MS	Leached (hot 6 M HCl)	Tl doping and sample-standard bracketing using NIST SRM 981 and values from Eisele et al. (2003)

Table A2. Comparison of new (re-analysed) and previously published Pb isotope data of Galunggung and Merapi volcanic rocks

Volcano/ Sample	Data source	$^{206}\text{Pb}/^{204}\text{Pb}$	$^{207}\text{Pb}/^{204}\text{Pb}$	$^{208}\text{Pb}/^{204}\text{Pb}$
Galunggung				
VB82	Turner and Foden (2001)	18.735	15.627	38.947
4AK	Turner and Foden (2001)	18.692	15.624	38.862
VB82	This study	18.799	15.699	39.194
4AK	This study	18.752	15.681	39.101
Merapi				
M97-68	Gertisser and Keller (2003a)	18.727	15.671	39.038
M96-137	Gertisser and Keller (2003a)	18.727	15.681	39.015
M96-73	Gertisser and Keller (2003a)	18.757	15.695	39.138
M98-96	Gertisser and Keller (2003a)	18.775	15.702	39.178
M95-26	Gertisser and Keller (2003a)	18.784	15.716	39.208
M97-68	This study	18.763	15.694	39.141
M96-137	This study	18.759	15.695	39.139
M96-73	This study	18.755	15.692	39.134
M98-96	This study	18.771	15.697	39.156
M95-26	This study	18.769	15.693	39.130

The previously published and new, re-analysed data for the same rock powders from Galunggung (VB82 and 4AK) show considerable variation in measured Pb isotope ratios (Table A2 and Fig. A1). The Galunggung Pb isotope ratios determined by Turner and Foden (2001) plot at significantly lower $^{207}\text{Pb}/^{204}\text{Pb}$ and slightly lower $^{206}\text{Pb}/^{204}\text{Pb}$ relative to both the new re-analysed data and the main Java array. The re-analysed Merapi samples show more similar Pb isotopic compositions to the previously published TIMS data of Gertisser and Keller (2003a) but the re-analysed data cover a more restricted range, particularly for $^{207}\text{Pb}/^{204}\text{Pb}$. The differences between the previously published TIMS data and our re-analysed MC-ICP-MS data for Galunggung and Merapi are likely due to: 1) the pre-treatment leaching in HCl for the re-analysed samples versus no leaching of the samples analysed by Turner and Foden (2001) and Gertisser and Keller (2003a) and 2) the conventional corrections employed for (unspiked) thermal ionisation mass spectrometer (TIMS) induced Pb-isotopic fractionation for the previously published data, versus TI-doping and MC-ICP-MS sample-standard bracketing for the re-analysed samples.

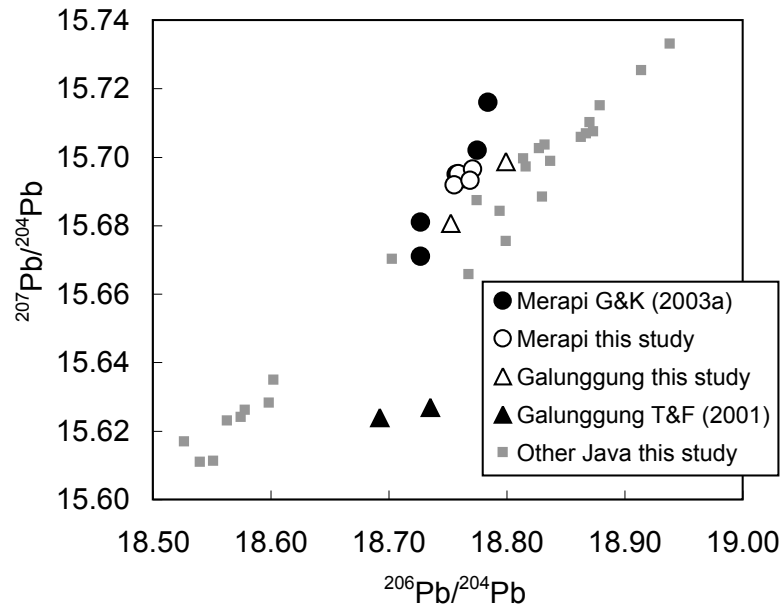


Fig. A1. Comparison of re-analysed and previously published Pb isotope data of Galunggung (Turner and Foden, 2001) and Merapi (Gertisser and Keller, 2003a) volcanic rocks. The new data for Gede, Salak and Ijen volcanoes (this study) are also plotted (grey symbols) for reference to the main Java array.

Selection of Javanese Pb isotope data sets for comparison

Due to the significant discrepancy observed between the previously published and re-analysed Galunggung Pb isotope data we have not used the Javanese Pb isotope data of Turner and Foden (2001) as a comparison data set in the manuscript. We use our re-analysed Pb isotope data for Merapi (instead of the Pb isotope data published by Gertisser and Keller, 2003a) in order for the data to be directly comparable to the new Merapi data presented in this study for the volcanic rocks erupted in 2006 and 2010. We note that as the Merbabu samples in this study were analysed using the same analytical methods and instrumentation of Gertisser and Keller (2003a) these data may also show a greater spread in $^{207}\text{Pb}/^{206}\text{Pb}$ relative to the new data presented for Merapi. Therefore, in the manuscript no attention has been drawn to the fact that the Merbabu Pb isotope data define an array of slightly different slope compared to the overall slope of the main Java array. The previously published Merapi data also presented a similar slope to Merbabu (compare the Merapi data of Fig. A2 with Merbabu data of Fig. 3c in the manuscript). The two Javanese data sets utilised for comparison in this study are Woodhead et al. (2001) (double-spiked TIMS data) and Edwards (1990) (conventional fractionation corrected TIMS data). Despite the latter study using a conventional fractionation correction, the Cereme and Guntur

data of Edwards (1990) plot along the main Java array and show the same slope (Fig. 3 of the manuscript). The older Javanese Pb isotope data set of Whitford (1975) has also been excluded from data comparison due to similar and significant discrepancies visible between the Whitford (1975) data and samples that were re-analysed by Woodhead et al. (2001).

Extended analytical techniques for the Tertiary sedimentary rocks of West Java

Major element contents of the three sedimentary whole-rock powders were determined on fused glass discs produced by the Fusion method (spectroflux 105) using the Automated Philips PW2404 X-ray fluorescence spectrometer at the University of Edinburgh. In-house rock standards were used to calibrate the machine and monitor accuracy and precision during analysis.

Trace element concentrations of the rock powders were determined on the PerkinElmer ELAN 6000 quadrupole ICP-MS at Durham University following the analytical procedure and instrument operating conditions described by Ottley et al. (2003). Multiple analyses of procedural blanks (3 per batch), in-house standards and international reference materials (W2, BHVO-1, AGV1, BE-N and BIR1) during each session (e.g. at the start, mid-way and at the end of a run) allowed for any drift in the instrument calibration to be detected. Reproducibility (internal and external) of standard values on the ELAN were better than 5% relative standard deviation.

Preparation of whole-rock powders for Sr, Nd and Hf isotope analysis was undertaken in the Arthur Holmes Isotope Geology Laboratory (AHIGL) at Durham University. The sample dissolution procedure and chemical separation of Sr, Hf and Nd from rock samples follow that presented by Dowall et al. (2003) and Handley et al. (2008a). Sr, Nd and Hf isotope ratios were determined on the AHIGL ThermoElectron Neptune MC-ICP-MS. Details of instrument operating conditions are presented in Nowell et al. (2003) and Dowall et al. (2003). Instrumental mass bias was corrected using $^{88}\text{Sr}/^{86}\text{Sr}$ of 8.375209 (the reciprocal of the $^{86}\text{Sr}/^{88}\text{Sr}$ ratio of 0.1194), $^{146}\text{Nd}/^{145}\text{Nd}$ of 2.079143 (equivalent to the more commonly used $^{146}\text{Nd}/^{144}\text{Nd}$ ratio of 0.7219) and $^{179}\text{Hf}/^{177}\text{Hf}$ of 0.7325 using an exponential law. Data quality was monitored over several analytical sessions by regular analysis of standard reference materials during each run. The reproducibility of $^{87}\text{Sr}/^{86}\text{Sr}$ for NBS 987 in each of the analytical sessions was better than 21 ppm. The reproducibility of $^{143}\text{Nd}/^{144}\text{Nd}$ and $^{176}\text{Hf}/^{177}\text{Hf}$ for the respective standard solutions in each of the analytical sessions was better than 19 and 28 ppm (2σ), respectively. The average reproducibility and accuracy of Nd and Hf isotope ratios of standard solutions over the period of

study are shown in Table B.3 (Appendix B) of Handley et al. (2010). Total procedural blanks (at least 2 processed per sample batch) were analysed by ICP-MS on the PerkinElmer ELAN 6000 quadrupole at Durham University and were below 1.2 ng (typically <300 pg), 219 pg and 73 pg, respectively, for Sr, Nd and Hf. These values are insignificant considering the quantity of Sr, Nd and Hf processed from the rocks.

References (not already given in the manuscript)

- Dowall, D. P., Nowell, G. M. and Pearson, D. G. (2003). Chemical pre-concentration procedures for high-precision analysis of Hf–Nd–Sr isotopes in geological materials by plasma ionisation multi-collector mass spectrometry (PIMMS) techniques. In: Holland, J. G. & Tanner, S. D. (eds) *Plasma Source Mass Spectrometry: Applications and Emerging Technologies*. Cambridge: Royal Society of Chemistry, pp. 321–337.
- Nowell, G.M., Pearson, D.G., Ottley, C.J., Schweiters, J. (2003). Long-term performance characteristics of a plasma ionisation multi-collector mass spectrometer (PIMMS): the ThermoFinnigan Neptune. *Plasma Source Mass Spectrometry*. Spec. Pub. Royal Soc. Chem., 307-320.
- Ottley, C.J., Pearson, D.G., Irvine, G.J. (2003). A routine method for the dissolution of geological samples for the analysis of REE and trace elements via ICP-MS. *Plasma Source Mass Spectrometry*. Spec. Pub. Royal Soc. Chem., 221-230.
- Todt, W., Cliff, R.A., Hanser, A., Hofmann, A.W. (1993). Re-calibration of NBS lead standards using a $^{202}\text{Pb}+^{205}\text{Pb}$ double spike. *Terra Abstr* 5:396.
- Thirlwall, M. F. (2000). Inter-laboratory and other errors in Pb isotope analyses investigated using a $^{207}\text{Pb}-^{204}\text{Pb}$ double spike. *Chemical Geology* 163, 299–322.
- Whitford, D.J. (1975). *Geochemistry and petrology of volcanic rocks from the Sunda arc, Indonesia*. Unpublished PhD Thesis, Australian National University.
- Woodhead, J.D., Hergt, J.M. (2000). Pb-isotopes analyses of USGS reference materials. *Geostandards Newsletter, The Journal of Geostandards and Geoanalysis* 24, 33-38.